Higgs mass and width measurements at ATLAS

PASCOS2024
20th Rencontres du Vietnam

July 9th, 2024

Laura Nasella (Università degli Studi & INFN Milano)
on behalf of the ATLAS Collaboration

Motivations behind the measurements 📚

m_H

The **Higgs boson mass** m_H is a fundamental free parameter of the Standard Model:

- the Higgs boson *production cross sections* σ and *decay branching ratios*, i.e. the Higgs boson **couplings** with all other particles, are established only when m_H is fixed
- m_H plays a key role in the **global EW fit**, i.e. in the internal consistency of the SM (interplay between the m_t, m_W and m_H)
- the **stability of the EW vacuum** depends on m_H

$\Rightarrow$ m_H **experimental measurement** needed!

Γ_H

The **Higgs boson width** Γ_H is predicted in the SM as a function of m_H: Γ_H ~ 4.1 MeV for m_H = 125 GeV.

Measurement needed to:

- Verify the SM predictions
- Solve the degeneracy between couplings and Γ_H: Higgs *production cross sections* as measured in different production and decay gives access to this ratio:

$$\boxed{\sigma_{i \to H \to f} = \frac{g_i^2 g_f^2}{\Gamma_H}}$$

where g_x is the modifier to H*xx* coupling

Higgs boson mass at ATLAS

$$\boxed{m_H}$$

The history of the mass measurement in ATLAS 📚

Previous measurements by ATLAS (CMS) with $H \to ZZ^* \to 4l$ and $H \to \gamma\gamma$ channels:

- **Full kinematic reconstruction** of the final state
- **Best invariant mass resolution** (1-2%) on the signal
- **Peak** above a continuum bkg in the $m_{\gamma\gamma}$ or m_{4l} distributions

	Analysis	**Precision** on m_H	
2012	Discovery	**0.45%**	Phys.Lett. B716 (2012) 1-29 — 126.0 ± 0.4 (stat.) ± 0.4 (syst.) GeV
2015	Run1 (25 fb^{-1} @ $\sqrt{s}$ = 7/8 TeV) ATLAS $H \to \gamma\gamma$	**0.4%**	Phys. Rev. Lett. 114, 191803 (2015)
2015	Run1 (25 fb^{-1} @ $\sqrt{s}$ = 7/8 TeV) ATLAS+CMS $\gamma\gamma + 4l$	**0.2%**	Phys. Lett. B 784 (2018) 345
2018	*Partial* Run2 (36 fb^{-1} @ $\sqrt{s}$ = 13 TeV) ATLAS $H \to \gamma\gamma$	**0.3%**	
2018	ATLAS $H \to 4l$	**0.3%**	
2022	Run2 ATLAS $H \to 4l$	**?%**	Analyses and results reported in today's presentation!
2023	Run2 ATLAS $H \to \gamma\gamma$; Run1 + Run2 ATLAS $\gamma\gamma + 4l$	**?%**	

Phys. Lett. B 843 (2023) 137880

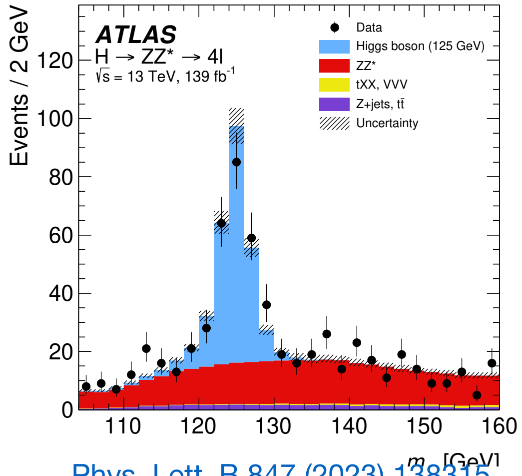

Phys. Lett. B 847 (2023) 138315

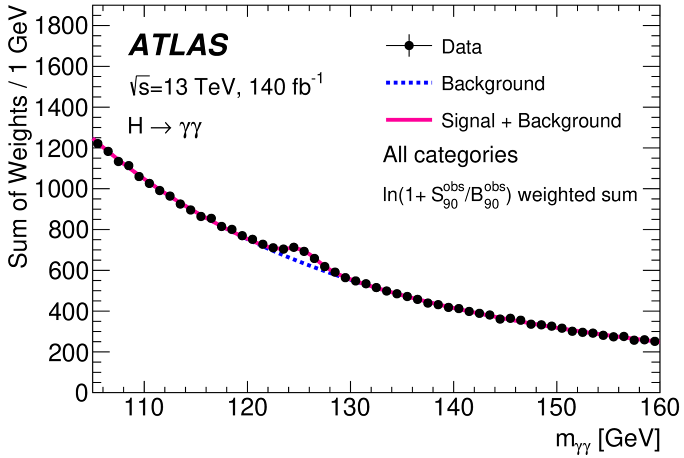

Electron, photon and muon calibration achievements 🏆

Why did it take **4/5 years** between the end of Run2 data taking (2018) and the full Run 2 mass results (2022/2023)?

2012

2015

2018 End of Run2

4/5 years

2022 Full Run2 results

2023

In-depth understanding of the **detector performance**, in particular regarding **e**, γ and μ

- **e/gamma:** JINST 19 (2024) P02009 backup slides 41-50
  - ✦ Larger datasets (Zee, Zllγ)
  - ✦ Updated/improved methods (LAr layer inter-calibration, uniformity corrections..)
  - ✦ **New linearity fit**: E_T dependent systematics are constrained by the measurement scale factors in E_T bins
  - ✦ Overall calibration uncertainty reduced by a factor of 2–3, depending on particle type η and p_T

- **muon:** Eur. Phys. J. C 83 (2023) 686 backup slides 52-58
  - ✦ New methodology charge-dependent sagitta bias scale correction
  - ✦ Inclusion of $J/\psi \to \mu\mu$ data in scale/reso correction
  - ✦ New fitting techniques with better convergence
  - ✦ Momentum scale uncertainty reduced up to a factor of 2

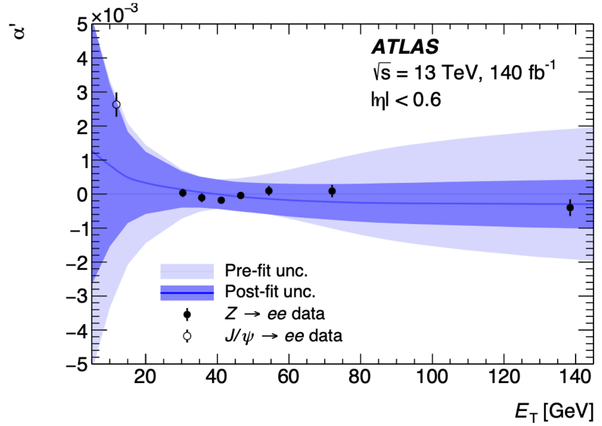

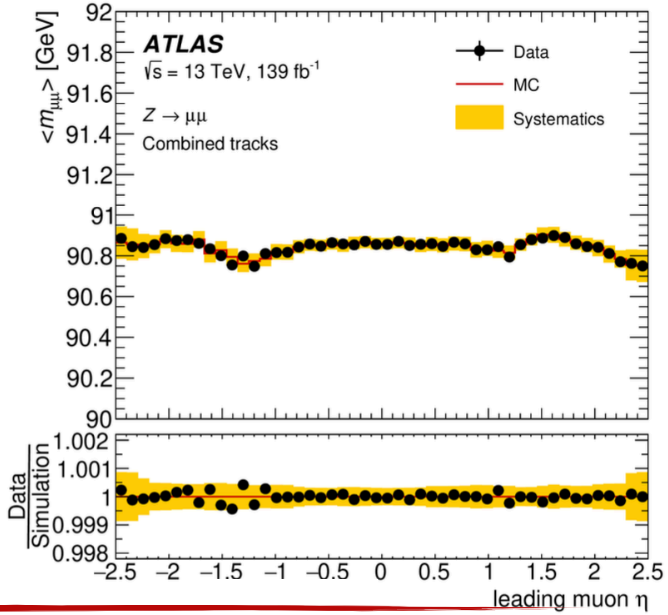

Mass measurement in the $H \to ZZ^* \to 4l$ channel

Phys. Lett. B 843 (2023) 137880

- Events containing at least four isolated leptons (l = *e*, μ) emerging from a common vertex, forming two pairs of oppositely charged same-flavour leptons.
- 4 channels: 4μ, 2μ2e, 2e2μ, 4e
- Dominant background = **non-resonant ZZ*** production (~90% of bkg yield)
- **Neural Network** based discriminant separating signal and background (D_{NN})
- Modelling of **per-event resolution** (σ_i)
  - The resolution ranges from 1.5 GeV (4μ and 2μ2e) to about 2.1 GeV (2e2μ and 4e)
- **Signal PDF** modelled as a function of D_{NN} , σ_i and m_{4l}

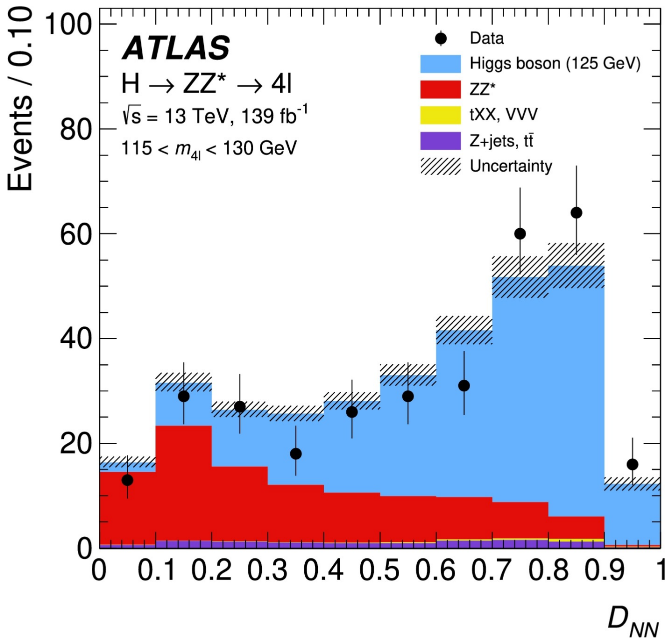

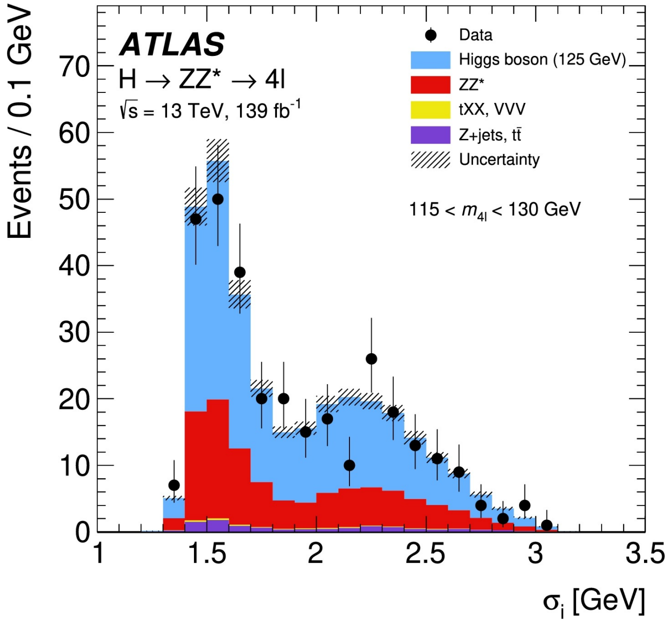

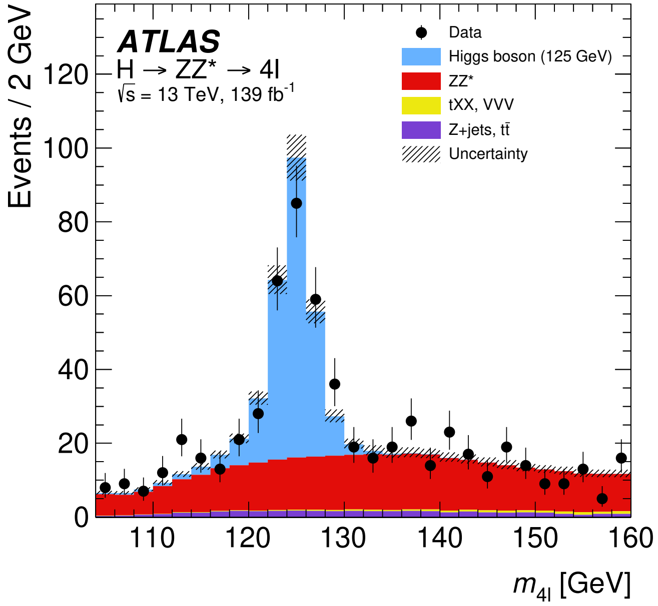

Mass measurement in the $H \rightarrow ZZ^* \rightarrow 4l$ channel

Phys. Lett. B 843 (2023) 137880

m_H from a simultaneous unbinned maximum-likelihood fit to the four channels in the mass range between 105 and 160 GeV

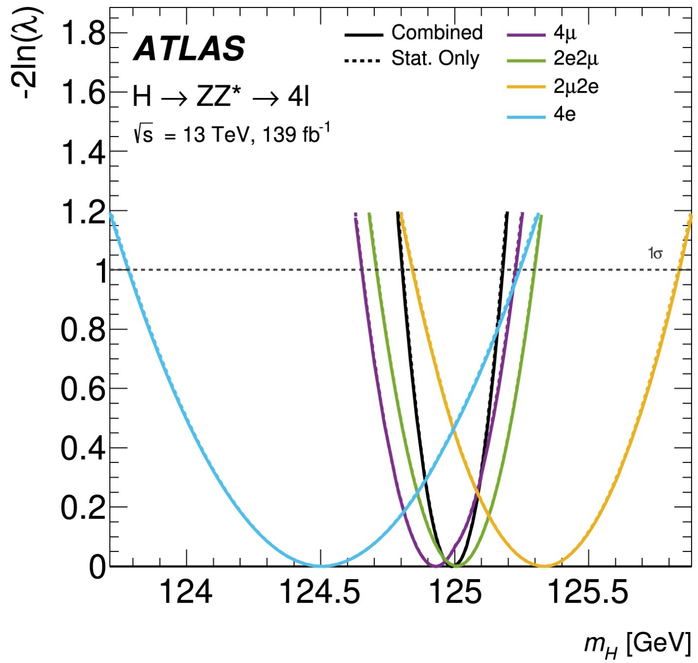

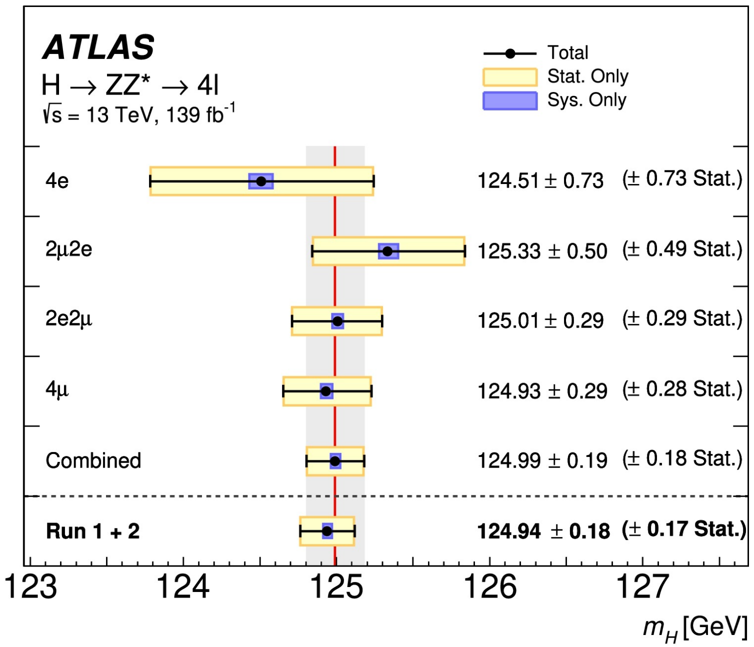

Systematic Uncertainty	Contribution [MeV]
Muon momentum scale	±28
Electron energy scale	±19
Signal-process theory	±14

- Statistically dominated
- Main syst. uncertainties from μ and $\boldsymbol{e}$ scale

0.15% precision

Run2 H→4l: m_H = 124.99 ± 0.18 (stat.) ± 0.04 (syst.) = 124.99 ± 0.19 GeV

Also performed combination with Run1 analysis:

0.14% precision

Run1+Run2 H→4l: m_H = 124.94 ± 0.17 (stat.) ± 0.03 (syst.) = 124.94 ± 0.18 GeV

Mass measurement in the $H \to \gamma\gamma$ channel

backup slides 24-38

Phys. Lett. B 847 (2023) 138315

- Require two good-quality and isolated photons with $p_T/m_{\gamma\gamma}$ > 0.35 (0.25)
- Separate events into 14 mutually exclusive **categories** to minimise the total expected uncertainty on m_H
- Model the **signal** and smoothly falling **background** with analytical functions

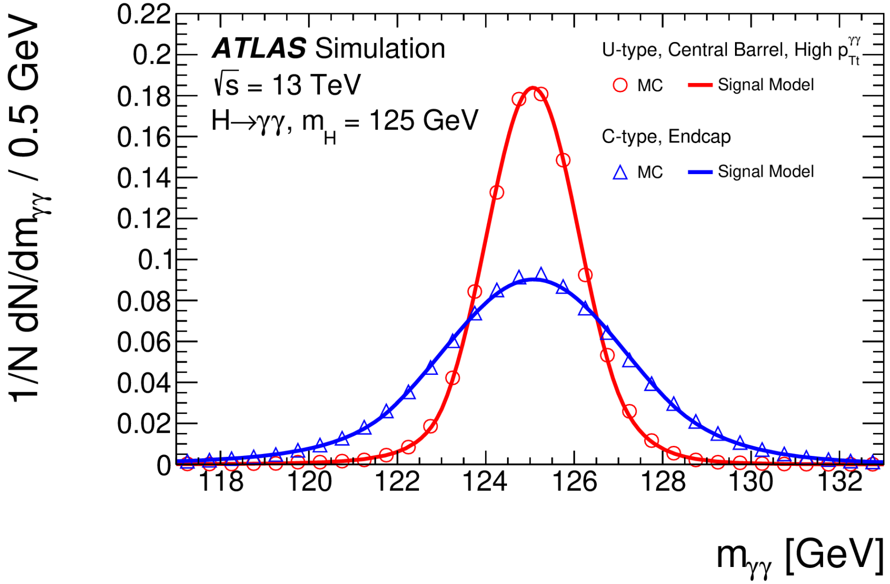

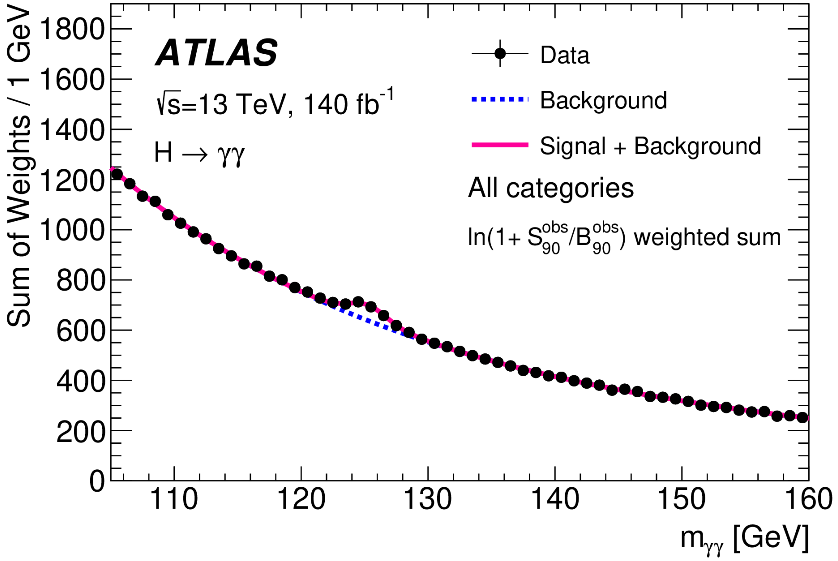

- **Systematic uncertainties** included in the model exploit new photon reconstruction with improved energy resolution and calibration
- Systematic uncertainty on m_H dominated by **photon energy scale**

Systematic uncertainty on m_H $(H \to \gamma\gamma)$		
Previous calibration	New calibration	New calibration + linearity
270 MeV	**180 MeV**	**83 MeV**

30% reduction

50% reduction

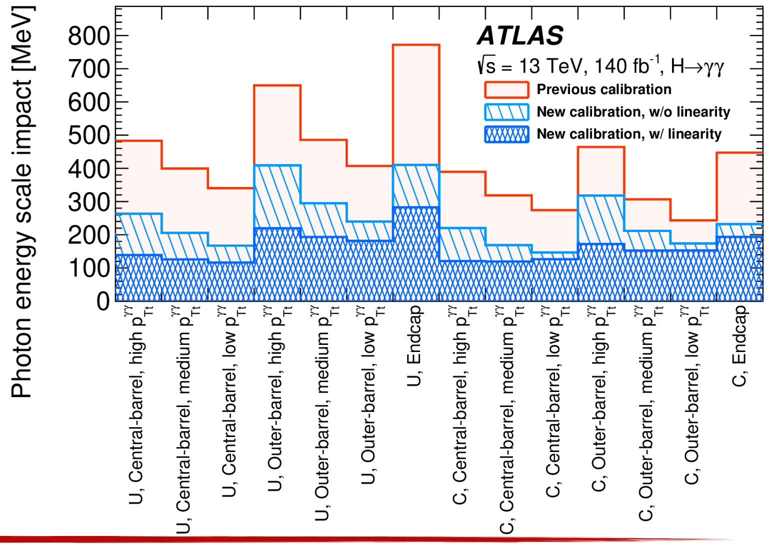

Mass measurement in the $H \to \gamma\gamma$ channel

Phys. Lett. B 847 (2023) 138315

- Require two good-quality and isolated photons with $p_T/m_{\gamma\gamma} > 0.35$ (0.25)
- Separate events into 14 mutually exclusive **categories** to minimise the total expected uncertainty on m_H
- Model the **signal** and smoothly falling **background** with analytical functions

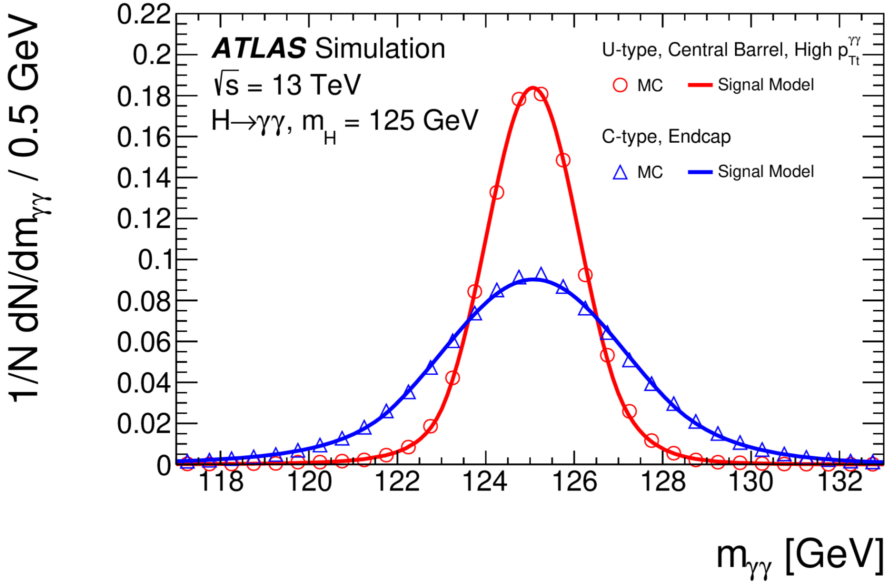

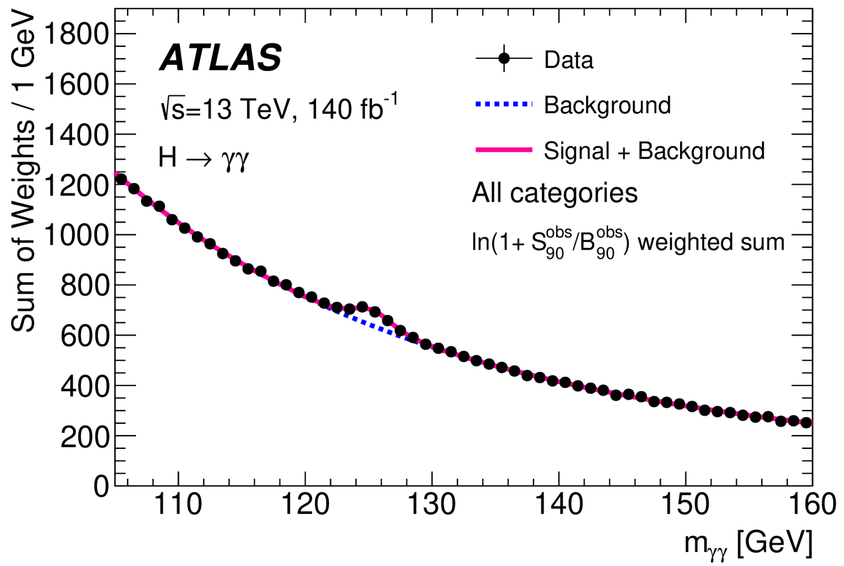

- **Systematic uncertainties** included in model as nuisance parameters, exploiting new photon reconstruction with improved energy resolution and calibration
- Systematic uncertainty on m_H dominated by **photon energy scale**
- **Interference** between the gg→H→γγ signal and the gg/qg→γγ background included as a systematic uncertainty
- Minor impact of signal and background modeling

Source	Impact [MeV]
Photon energy scale	83
$Z \to e^+e^-$ calibration	59
E_T-dependent electron energy scale	44
$e^\pm \to \gamma$ extrapolation	30
Conversion modelling	24
Signal–background interference	26
Resolution	15
Background model	14
Selection of the diphoton production vertex	5
Signal model	1
Total	90

Mass measurement in the $H \rightarrow \gamma\gamma$ channel

[Phys. Lett. B 847 (2023) 138315]

m_H from a simultaneous maximum-likelihood fit to the 14 categories in the mass range between 105 and 160 GeV

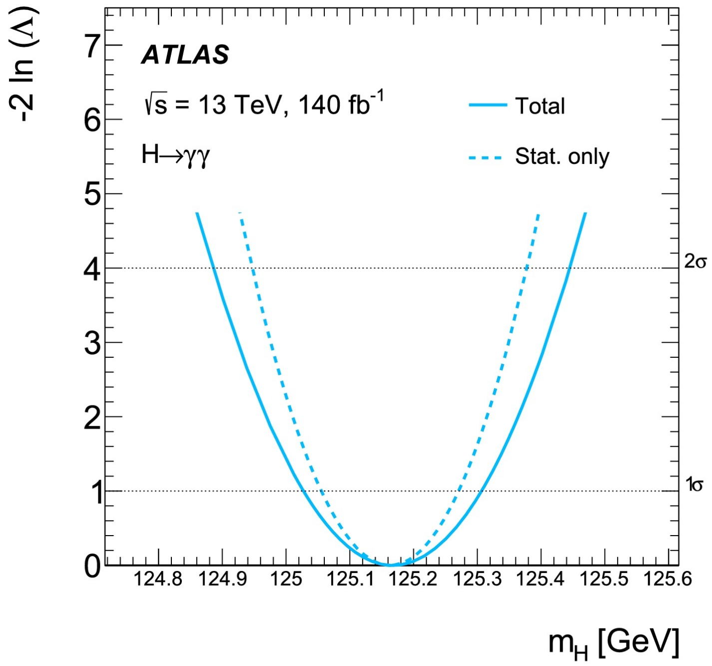

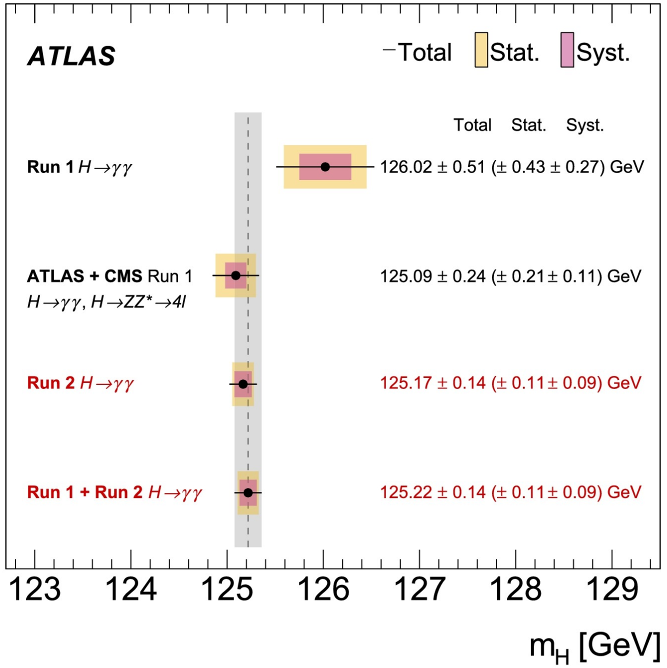

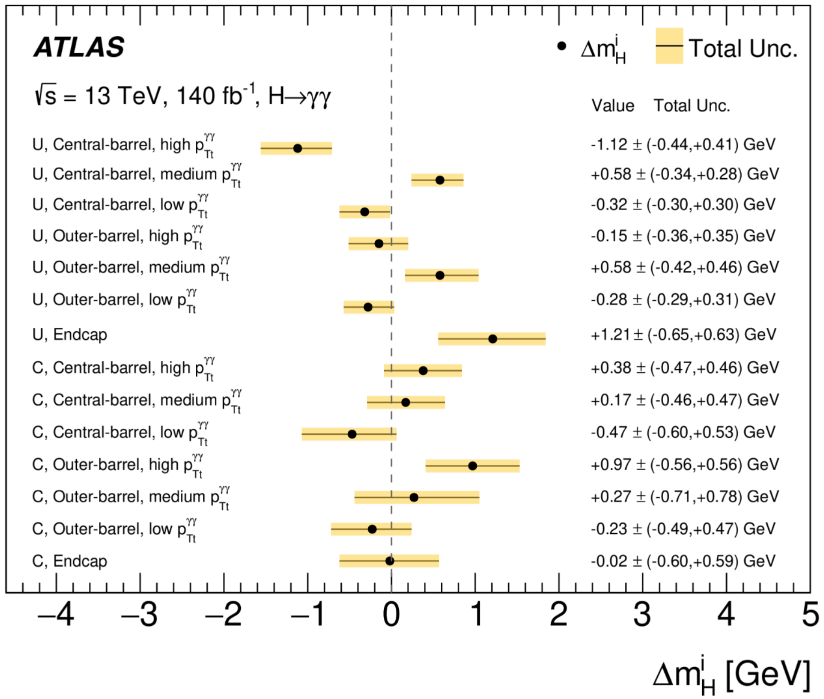

Run2 $H \rightarrow \gamma\gamma$: m_H = 125.17 ± 0.11 (stat.) ± 0.09 (syst.) = 125.17 ± 0.14 GeV

Also performed combination with Run1 analysis:

0.11% precision

Run1+Run2 $H \rightarrow \gamma\gamma$: m_H = 125.22 ± 0.11 (stat.) ± 0.09 (syst.) = 125.22 ± 0.14 GeV

Now stat. dominated

$H \rightarrow \gamma\gamma$ + $H \rightarrow 4l$ Run1-Run2 combination 🥇

Phys. Rev. Lett. 131 (2023) 251802

	Fitted m_H	Uncertainty [GeV] Total	Stat.	Syst.	Fitted m_H	Uncertainty [GeV] Total	Stat.	Syst.	Fitted m_H	Uncertainty [GeV] Total	Stat.	Syst.
	H→γγ				**H→4l**				**Combination: ≠ channel, = Run**			
Run1	126.02	0.51	0.44	0.27	124.51	0.53	0.53	0.03	125.38	0.43	0.39	0.19
Run2	125.17	0.14	0.11	0.09	124.99	0.18	0.18	0.03	125.10	0.11	0.09	0.07
Combination: = channel, ≠ Run	125.22	0.14	0.11	0.09	124.94	0.18	0.17	0.03	**125.11**	**0.11**	**0.09**	**0.06**

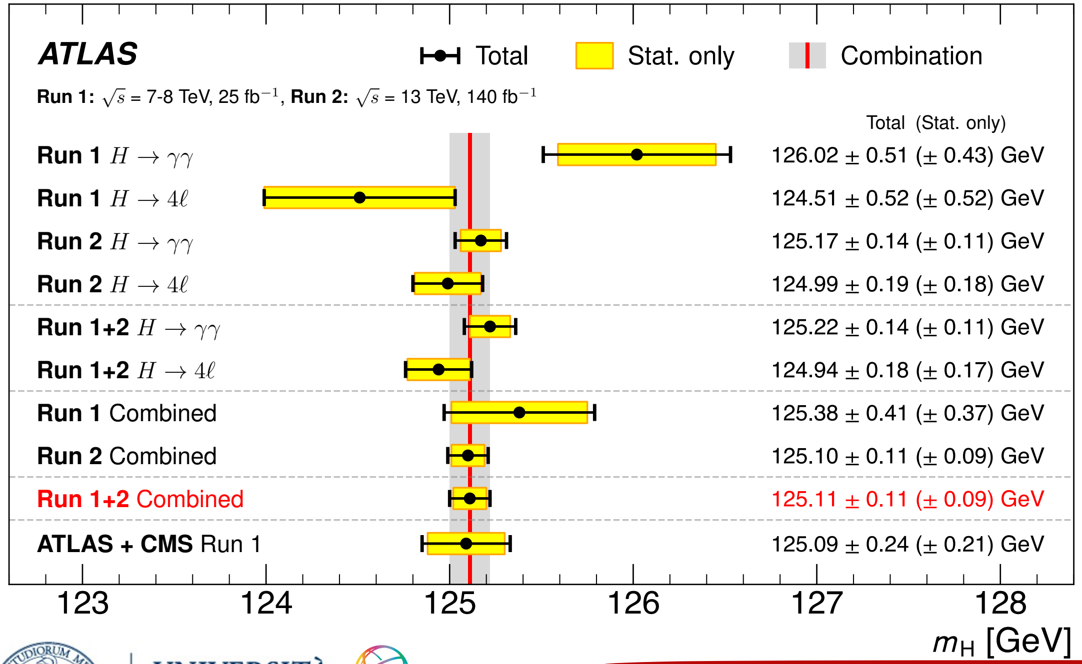

Run1+Run2 comb: m_H = 125.11 ± 0.11 GeV = 125.11 ± 0.09 (stat.) ± 0.06 (syst.)

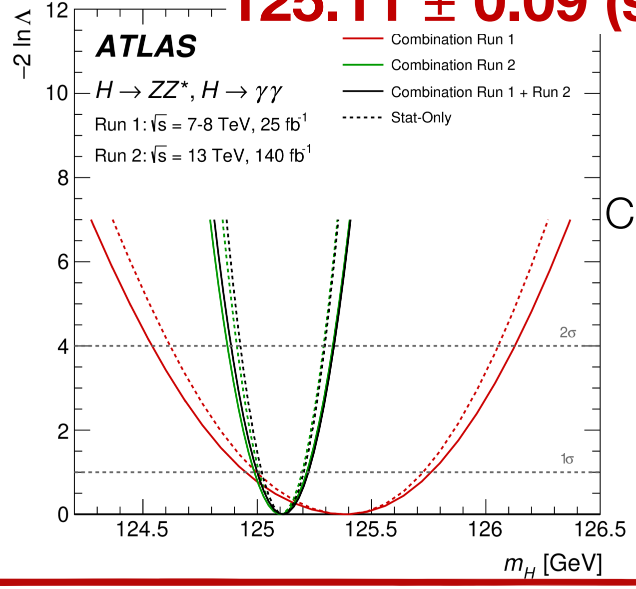

Current **most precise measurement** of m_H

Total uncertainty ∼ 110 MeV

< 1‰ precision!! 🥳

Higgs boson width at ATLAS

$$\boxed{\Gamma_H}$$

Measurement of the Higgs boson width

Phys. Lett. B 846 (2023) 138223

SM predicts the Higgs boson **width** of Γ_H = 4.1 MeV ⇒ too small for direct on-shell measurement!

- **gg→H→ZZ** final state: production cross-section as a function of the invariant mass of the four leptons m_{4l}

$$\frac{d\sigma_{pp\to H\to ZZ}}{dm^2_{4l}} \sim \frac{g^2_{Hgg}g^2_{HZZ}}{(m^2_{4l}-m^2_H)^2+m^2_H\Gamma^2_H}$$

$$\sigma^{\text{on-shell}}_{gg\to H\to ZZ^*} \sim \frac{g^2_{Hgg}g^2_{HZZ}}{m_H\Gamma_H}$$ **on-shell**, $m_{ZZ} \sim m_H$

$$\sigma^{\text{off-shell}}_{gg\to H^*\to ZZ} \sim \frac{g^2_{Hgg}g^2_{HZZ}}{m^2_{4l}}$$ **off-shell**, $m_{ZZ} \gg m_H$

Eur. Phys. J. C (2015) 75:335

- Assuming that the on-shell and off-shell Higgs production follow SM prediction (the H_{gg} and H_{ZZ} coupling modifiers are the same on-shell and off-shell), Γ_H can be measured (indirectly) from the ratio of **off-shell/on-shell** Higgs boson cross sections

$$\boxed{\Gamma_H \propto \frac{\sigma^{\text{off-shell}}_{gg\to H^*\to ZZ}}{\sigma^{\text{on-shell}}_{gg\to H\to ZZ^*}}}$$

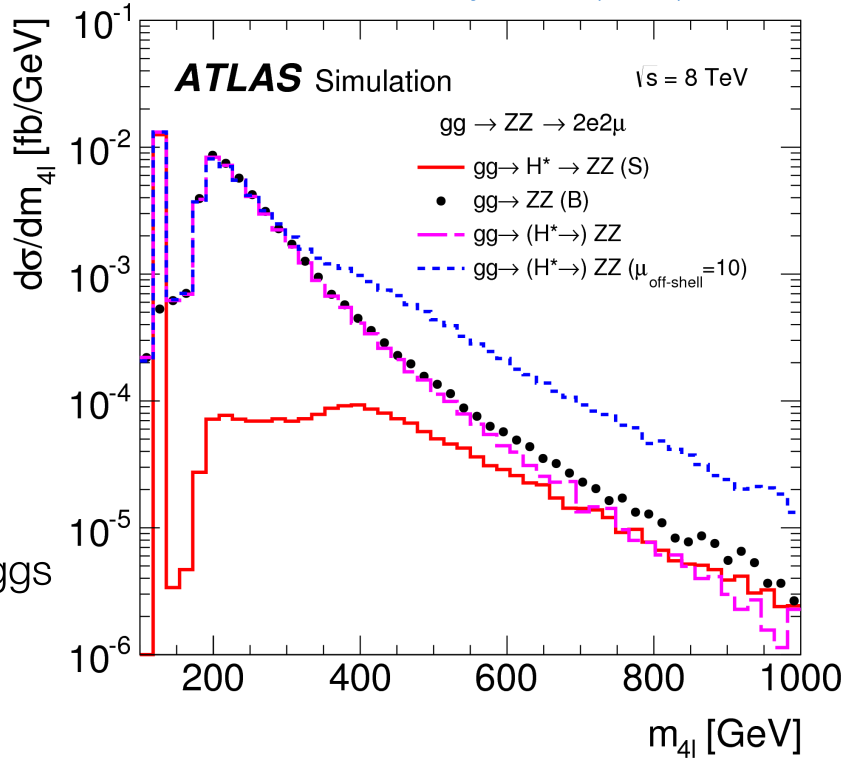

In SM the total impact of the H is negative ⇒ off-shell Higgs manifestation = deficit of events w.r.t. background only expectation

Measurement of the Higgs boson width

Phys. Lett. B 846 (2023) 138223

Measuring the **off-shell** contribution not straightforward: **interference** with continuum background

- **Gluon-gluon (ggF) production**

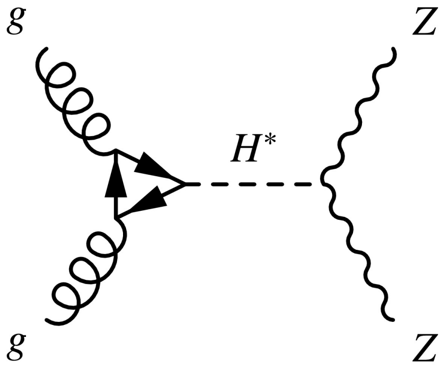

ggF signal (S)

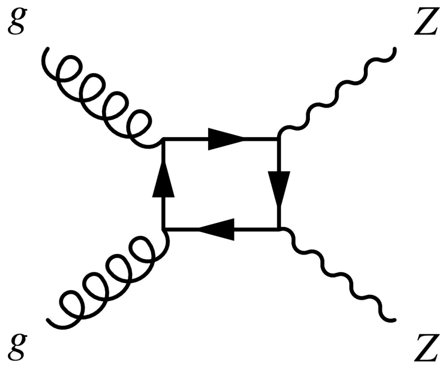

gg→ZZ background (B)

Interference (I)

$$N_{gg\to(H^*)\to ZZ} = \mu_{\text{off-shell}} N_S + \sqrt{\mu_{\text{off-shell}}}\,(N_{S+B} - N_S - N_B) + N_B$$

- **Electroweak EW (VBF+VH) production**

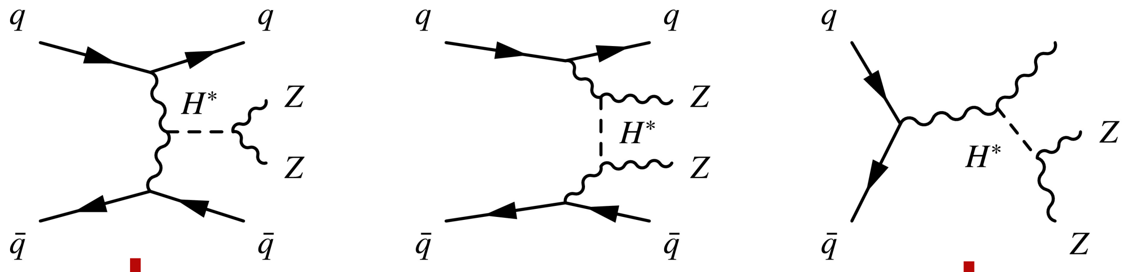

EW signal (S)

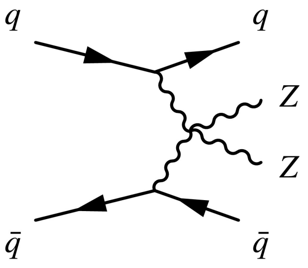

EW background (B)

Measurement of the Higgs boson width

Phys. Lett. B 846 (2023) 138223

The measurement is performed considering two final states:

- $ZZ \rightarrow 4l$: clean and fully reconstructed final state
- $ZZ \rightarrow 2l2\nu$: six times higher branching ratio

Targeting off-shell contribution from both **ggF** and **EW** (VBF+VH) modes

- Three signal regions (SR) are defined after requiring $m_{4l} > 220$ GeV. Events separated in:
  - electroweak-like (require two or more jets with $p_T > 30$ GeV and $|\Delta\eta_{jj}| > 4$),
  - mixed categories = require exactly one jet with $|\eta_j|>2.2$
  - ggF-like = remaining events
- Normalization of non-interfering background from $qq \rightarrow ZZ$ fitted on data CR

Signal vs bkg discriminated using **NN** (*4l*) or **transverse mass** (2l2v)

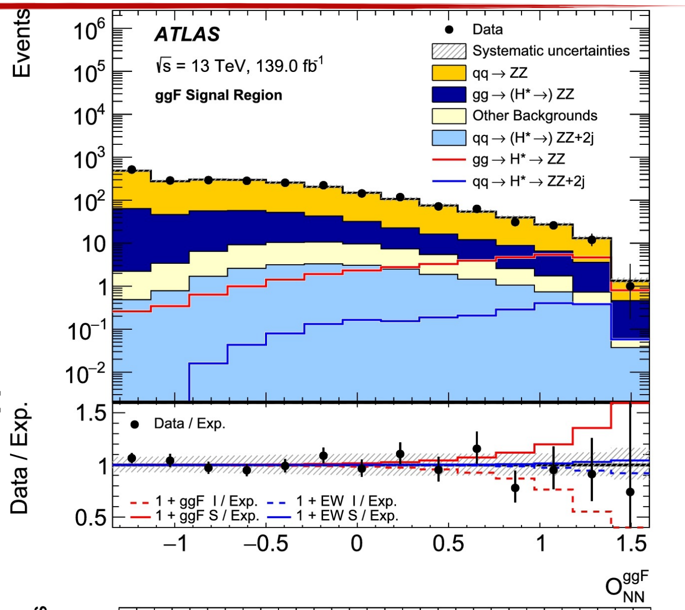

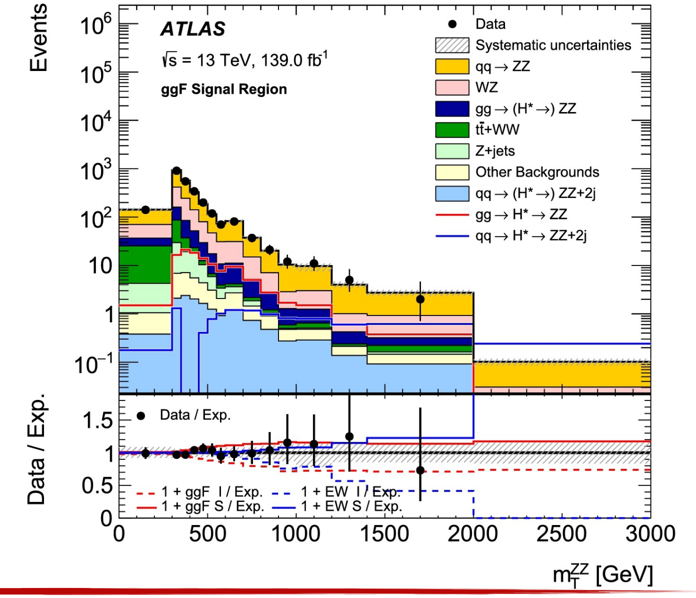

Measurement of the Higgs boson width

[Phys. Lett. B 846 (2023) 138223]

- Simultaneous fit **signal strength** and **background normalization factors** in all signal regions and control regions
- Direct measurement of off-shell signal strength $\mu_{\mathrm{off-shell}}$

$\mu_{\text{off-shell}} = 1.1 \pm^{0.7}_{0.6}$

with a significance of off-shell production 3.3 (2.2) σ

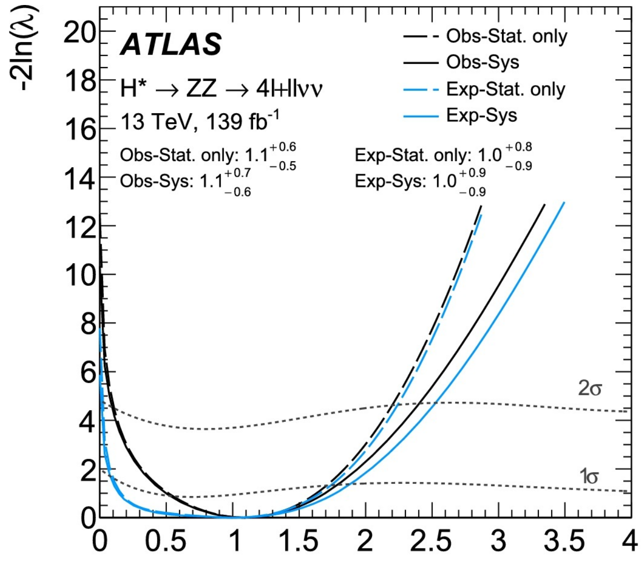

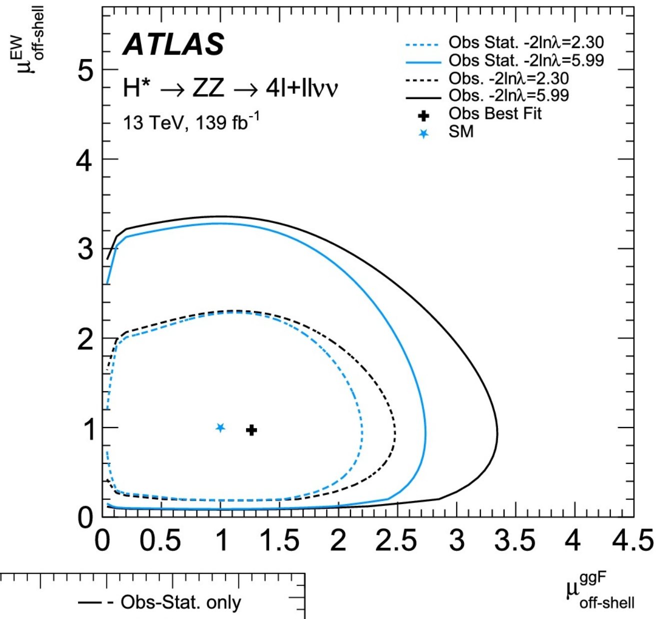

- Combining the off-shell with on-shell $H \to ZZ^* \to 4l$ measurement to measure Γ_H with correlated (uncorrelated) experimental (theoretical) systematic uncertainties

$$\boxed{\Gamma_H = 4.5 \pm^{3.3}_{2.5}\ \text{MeV}}$$

and 0.5 (0.1) < Γ_H < 10.5 (10.9) MeV at 95% CL

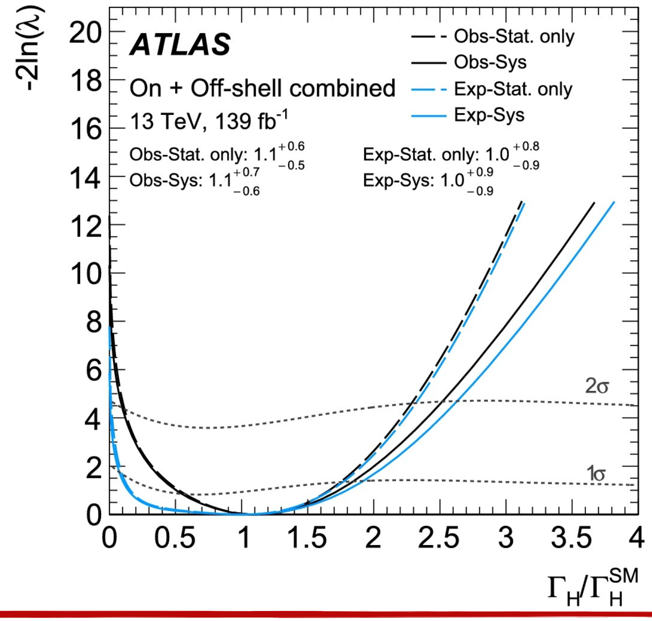

Conclusions 🎯

- ATLAS made huge efforts in improving the understanding of the detector's performance during Run 2 (140 fb^{-1} at 13 TeV of centre-of-mass energy) allowing improvements in m_H uncertainty

- The new ATLAS measurements of the Higgs boson mass by combining $H\rightarrow\gamma\gamma$ and $H\rightarrow ZZ^*\rightarrow 4l$ final states and using $\sqrt{s}$=7,8 and 13 TeV data, resulted in the current most precise m_H measurement with an uncertainty of 0.09%:

Run1+Run2 comb: m_H = 125.11 ± 0.11 GeV = 125.11 ± 0.09 (stat.) ± 0.06 (syst.)

- The determination of the Higgs boson width Γ_H is very hard at hadron colliders: exploiting the ratio of off-shell to on-shell Higgs boson production in the ZZ decay channel with reasonable assumptions, ATLAS measured the Higgs boson width:

$\Gamma_H = 4.5 \pm^{3.3}_{2.5}$ MeV, and 0.5 (0.1) < Γ_H < 10.5 (10.9) MeV at 95% CL

Thank you for your attention!
cảm ơn!

Backup

The Standard Model Higgs boson

- The Standard Model (SM) of particle physics is a quantum field theory:
  - classify all the known elementary particles
  - describe strong and electroweak interactions: $SU(2)_L \times U(1)_Y \times SU(3)_C$

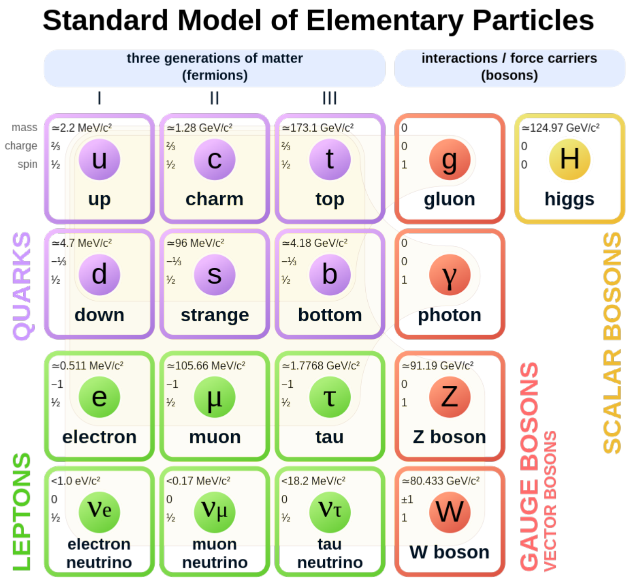

Problem: The introduction of mass terms for the gauge bosons $W^{\pm}$ and Z in the SM Lagrangian would **violate** the local gauge invariance of the theory.

Solution: the ***Higgs mechanism*** (1964) and the *spontaneous symmetry breaking* allow to give mass to the particles dynamically, through the interaction with a scalar field Φ. Self-interaction term through $V(\Phi)$:

$$V(\Phi) = \lambda(\Phi^\dagger\Phi)^2 - \mu^2(\Phi^\dagger\Phi)$$

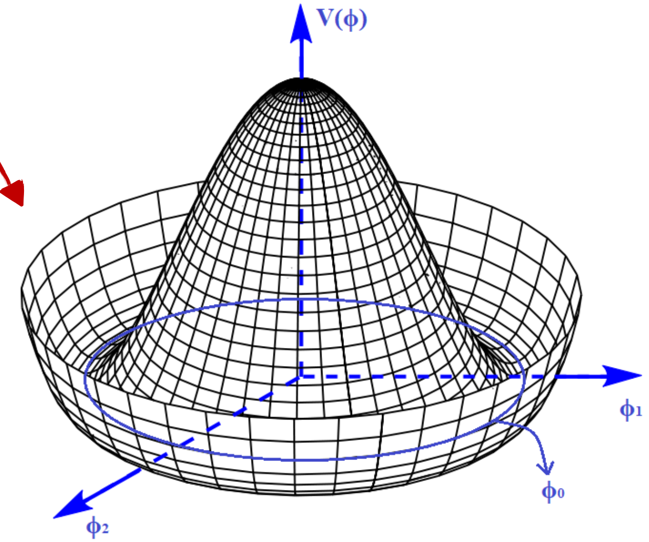

$V(\Phi)$ has infinite minima → Φ aquires one ground state → this choice *spontaneously break the symmetry* of the configuration → mass terms arise! ✅

- The quantum of the field is the **Higgs boson** H, a massive scalar particle

Production cross sections and decay Branching ratios

- **Cross sections:** considering $\sqrt{s}$ = 13 TeV and m_H ~ 125 GeV, the total cross section is σ_H~56 pb

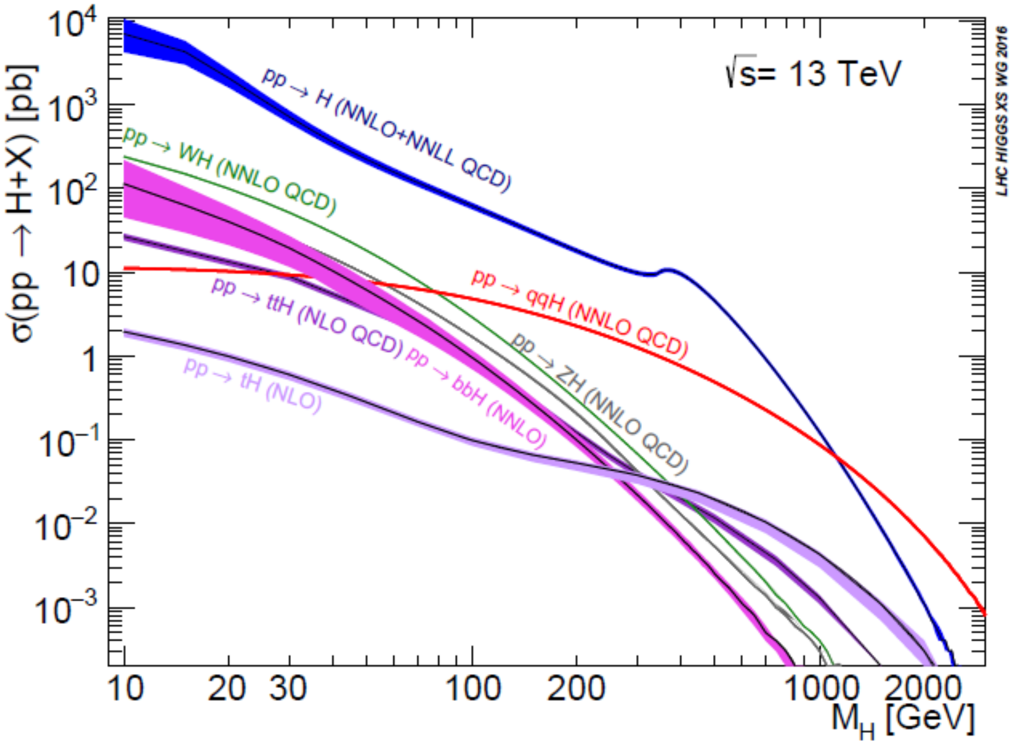

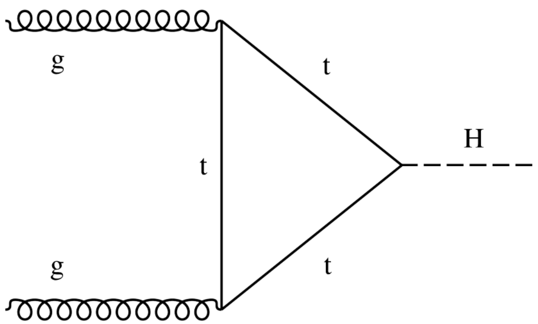

ggF, σ_{ggF}~48.5 pb

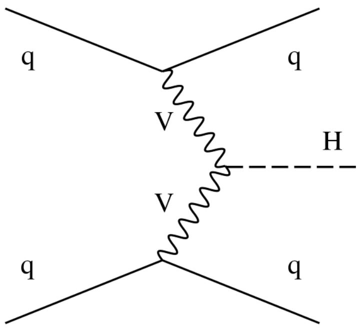

VBF, σ_{VBF}~3.8 pb

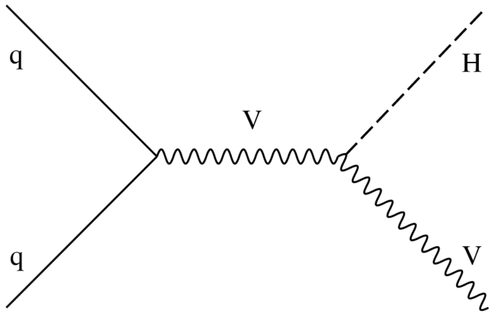

VH = WH or ZH, σ_{WH}~1.4 pb

σ_{ZH}~0.88 pb

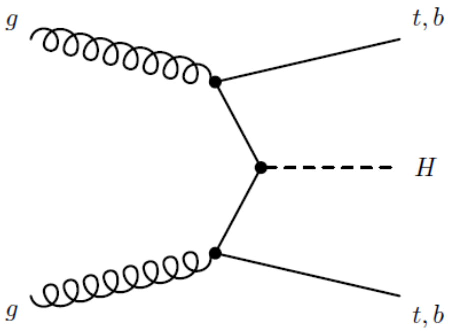

$t\bar{t}$H and $b\bar{b}$H, σ_{ttH}~0.51 pb

σ_{bbH}~0.49 pb

Production cross sections and decay Branching ratios

- **Branching ratios:** $BR\left(H \to X_i\right) = \dfrac{\Gamma(H \to X_i)}{\sum_i \Gamma(H \to X_i)}$

  - H ⟶ $b\bar{b}$: BR ~ 58.1 %
  - H ⟶ WW*(⟶lνlν): BR ~ 21.5 %
  - …
  - H ⟶ ZZ*: BR ~ 2.6 %
    ZZ*⟶ 4l: BR ~ 0.0125%
  - H ⟶ γγ: BR ~ 0.227%

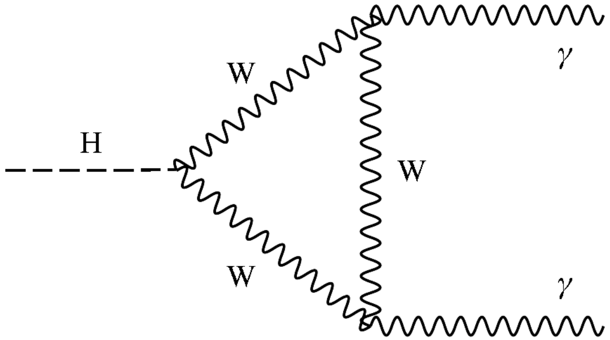

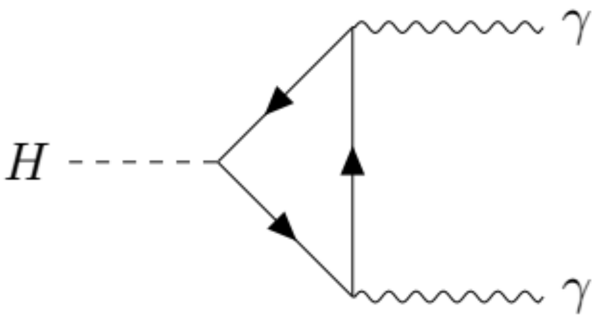

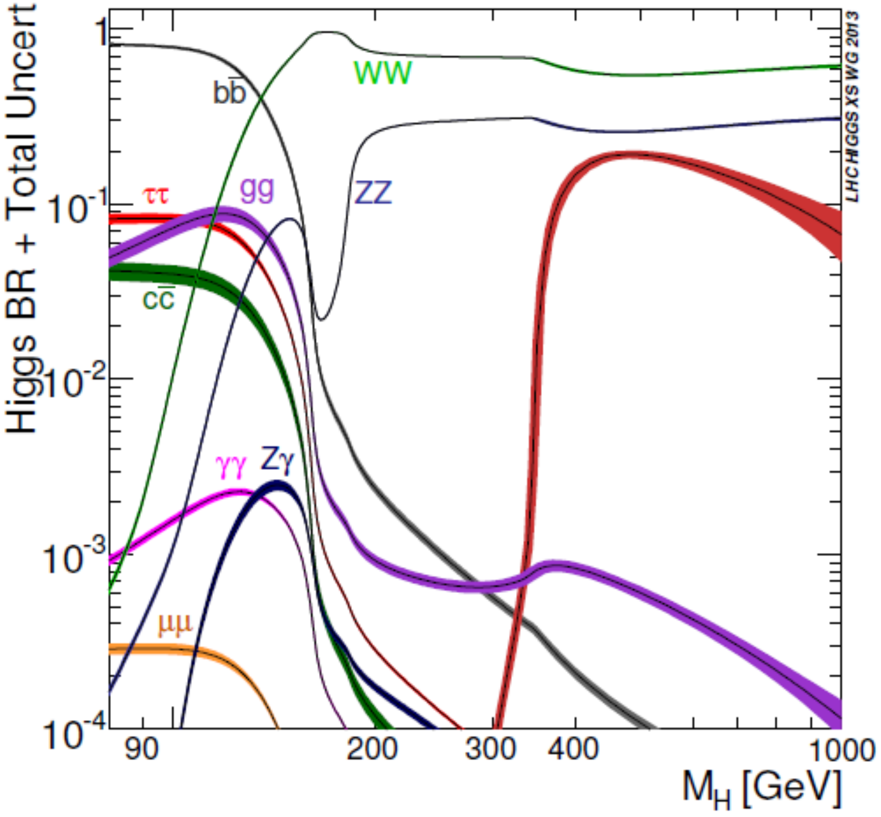

Vacuum stability and EW fits

- **Vacuum stability**: The value of the Higgs mass determines the vacuum stability, i.e. the Higgs potential might be unbounded below or exhibit lower additional minima given a certain m_H below the Planck scale

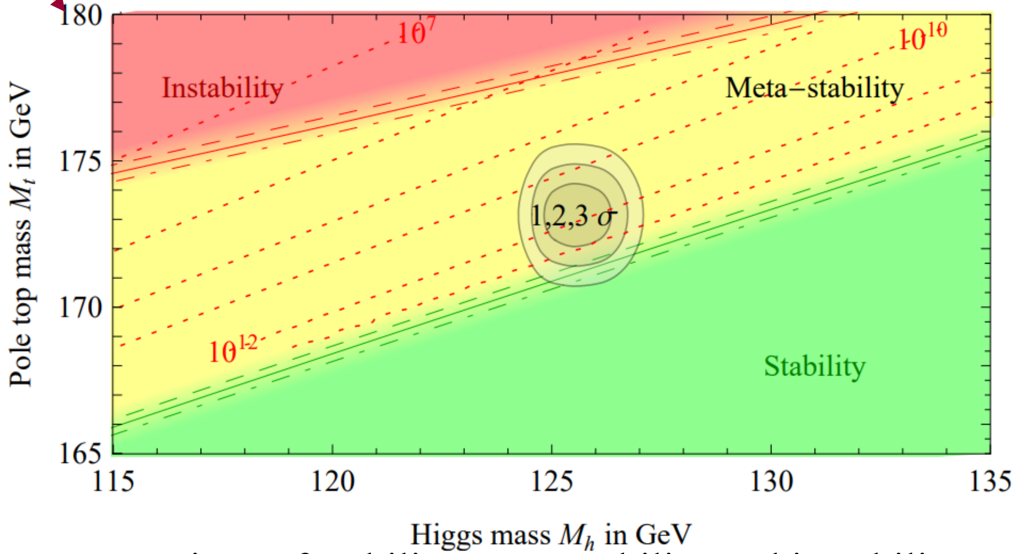

Regions of stability, meta-stability and instability of the SM vacuum in the m_t - m_H plane

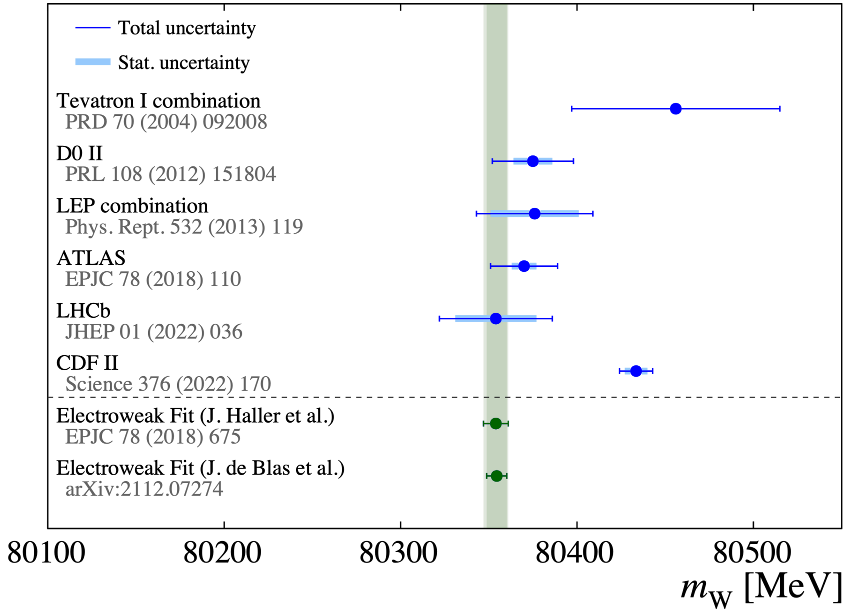

- **Global EW fits**: they test the internal consistency of the SM. The SM prediction of the W gauge boson mass m_W from the electroweak fit including the Higgs boson mass as input, gives $m_W = 80.354 \pm 0.007$ GeV. This theoretical result is compatible with ATLAS measurement but in severe tension (7σ) with CDF result of $m_W = 80.43350 \pm 0.0094$ GeV

Higgs boson mass at ATLAS

$$\boxed{\mathbf{H} \rightarrow \gamma\gamma}$$

$H \to \gamma\gamma$ Run 2: analysis strategy

- **Data samples**: full **Run 2** (2015-2018) *pp* dataset collected by ATLAS at $\sqrt{s}$ = **13 TeV** for a total integrated luminosity of **L = 140 fb^{-1}**
- **Purpose**: measure m_H from the position of the resonant signal
- **Event selection** aimed at reducing the γ-jet and di-jet bkg by looking for two tight and isolated good-quality photons

1) Event **categorisation** optimised to reduce the total exp. uncertainty on m_H
2) Analytical **signal** model $\propto m_H$, $\forall$ category
3) Analytical **background** model $\forall$ category
4) Experimental **systematic** uncertainties (PES)
5) Modelling + secondary systematic uncertainties
6) **Statistical model**, expected and observed results
   - Maximum likelihood simultaneous fit over the categories on data
   - m_H value and errors from a likelihood scan
7) Run1 - Run2 $H \to \gamma\gamma$ **combination**

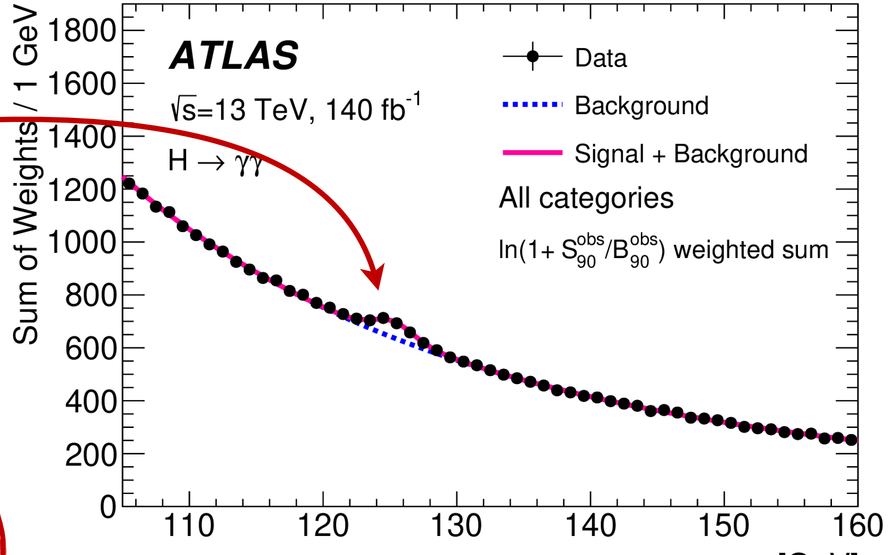

Phys. Lett. B (2023) arXiv:2308.07216

Event selection requirements	
Diphoton triggers	2015-2016: HLT_g35_loose_g25_loose + HLT_g120_loose 2017-2018: HLT_g35_medium_g25_medium + HLT_g140_loose
Photons preselection	Loose ID, p_T > 25 GeV, $\lvert\eta\rvert$ < 2.37 avoiding crack region
Diphoton Neural Network vertex	Increase vertex classification efficiency and diphoton $m_{\gamma\gamma}$ resolution up to 8%
Photon final selection	Tight ID, FixedCutLoose isolation, $p_T^{\gamma}/m_{\gamma\gamma}$ >0.25(0.35), $m_{\gamma\gamma}$ in [105,160] GeV

1) $H \to \gamma\gamma$ Run 2: categorization

Purpose: divide events into mutually exclusive categories optimized to **reduce the total uncertainty** on m_H

- Categories targeting different $m_{\gamma\gamma}$ **resolution**, **PES systematics** and **S/B ratios**
- Many different schemes tested, compared with a full shape model + PES uncertainties

Categorization scheme: **14** categories based on γ **kinematic variables** as **η**, **p_{Tt}** and conversion status

- Conversion status: 0 (U-type) or ≥ 1 (C-type) converted γ
- Pseudorapidity |η|: - Central-barrel (both γ |η| < 0.8)
  - Outer-barrel (≥ 1 γ in 0.8 < |η| < 1.37 & not in Endcap)
  - Endcap (≥ 1 γ in 1.52 < |η| < 2.37)
- p_{Tt}: High/Medium/Low bins defined by 70 and 130 GeV boundaries

Gain on total m_H uncertainty from categorization:

- -17% compared to inclusive measurement (1 category)
- -6% compared with partial Run 2 analysis @ 36 ifb (31 categories)

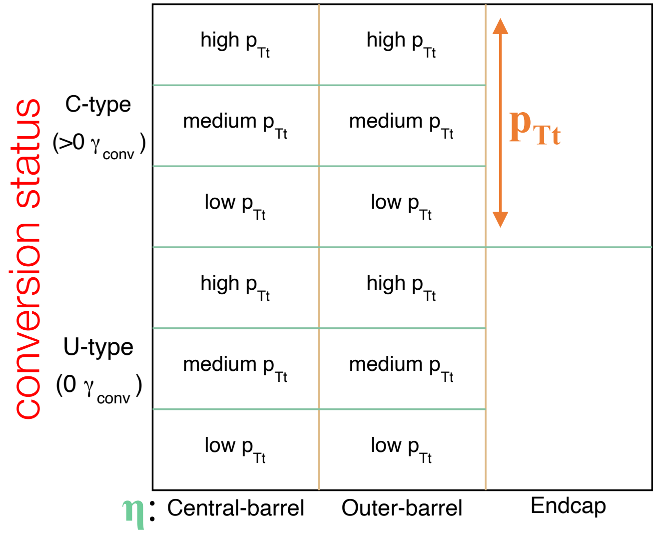

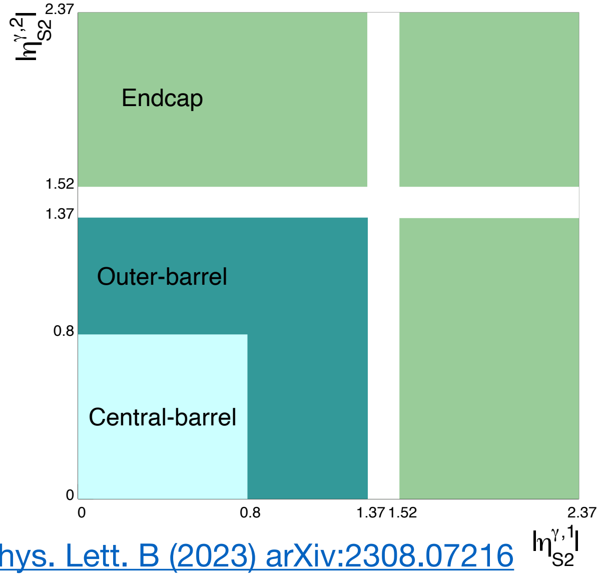

Phys. Lett. B (2023) arXiv:2308.07216

1) $H \rightarrow \gamma\gamma$ Run 2: categorization

[Phys. Lett. B (2023) arXiv:2308.07216]

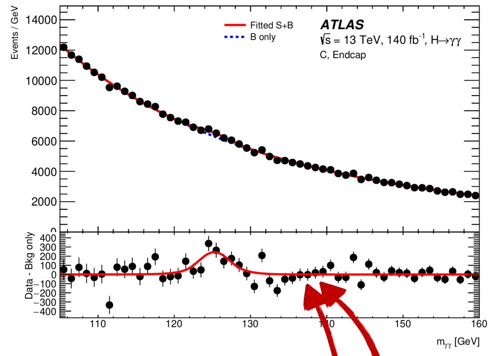

Purpose: divide events into mutually exclusive categories optimized to **reduce the total uncertainty** on m_H

- Categories targeting different $m_{\gamma\gamma}$ **resolution**, **PES systematics** and **S/B ratios**
- Many different schemes tested, compared with a full shape model + PES uncertainties

Lowest systematics

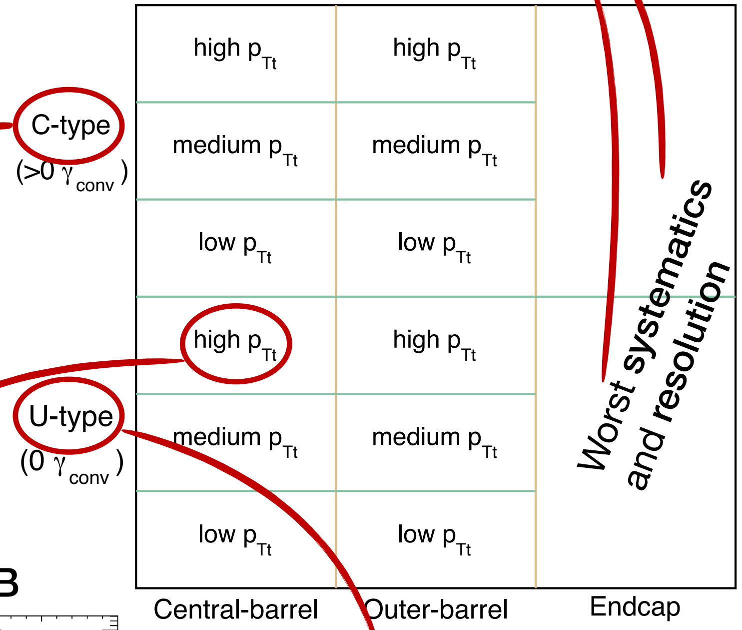

Categorization scheme: **14** categories based on γ **kinematic variables** as **η**, **p_{Tt}** and conversion status

- Conversion status: 0 (U-type) or $\geq$ 1 (C-type) converted γ
- Pseudorapidity |η|: - Central-barrel (both γ $|\eta| < 0.8$)
  - Outer-barrel ($\geq$ **1** γ in $0.8 < |\eta| < 1.37$ & not in Endcap)
  - Endcap ($\geq$ **1** γ in $1.52 < |\eta| < 2.37$)
- **p_{Tt}**: High/Medium/Low bins defined by 70 and 130 GeV boundaries

Good **S/B**

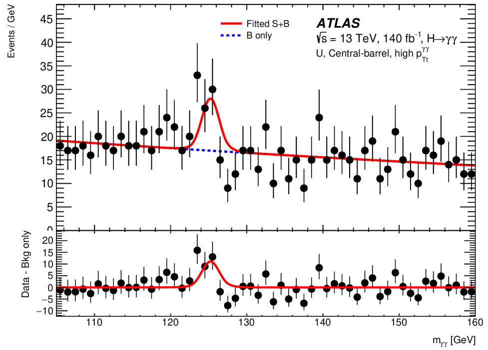

Best **resolution**

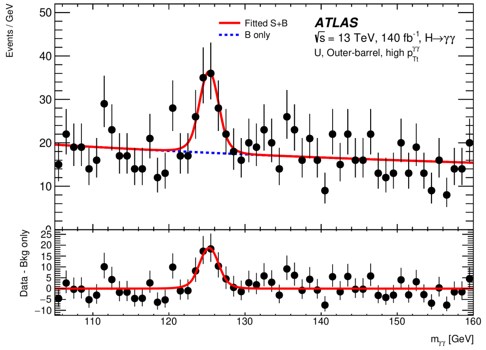

Gain on total m_H uncertainty from categorization:

- -17% compared to inclusive measurement (1 category)
- -6% compared with [partial Run 2 analysis @ 36 ifb] (31 categories)

2) $H \to \gamma\gamma$ Run 2: signal model $\propto m_H$

- Using **simulated signal Monte Carlo samples** at 9 different m_H values: from 110 to 140 GeV
- The $m_{\gamma\gamma}$ distribution of the resonant signal process is modelled with a **Double-Sided Crystall Ball** (DSCB) function: gaussian peak (μ_{CB}, σ_{CB}) and power-law tails
- To obtain the dependence of the signal shape on m_H, the parameters of the DSCB are parametrised as function of m_H $\forall$ category: simultaneous fit over the 9 MC samples to obtain the parameters values
- Signal model extensively **cross-checked** internally: most extreme impact on m_H always ≤ 15 MeV

$$\mu_{CB}(m_H) = m_H + B_{\mu_{CB}} + A_{\mu_{CB}}(m_H - 125\ \text{GeV})$$
$$\sigma_{CB}(m_H) = B_{\sigma_{CB}} + A_{\sigma_{CB}}(m_H - 125\ \text{GeV})$$
$$\alpha_{Low}(m_H) = \alpha_{Low} \qquad \alpha_{High}(m_H) = \alpha_{High}$$
$$n_{Low}(m_H) = n_{Low}|_{125\text{GeV}} \qquad n_{High}(m_H) = n_{High}|_{125\text{GeV}}$$

Example of simultaneous fit for 1 category:

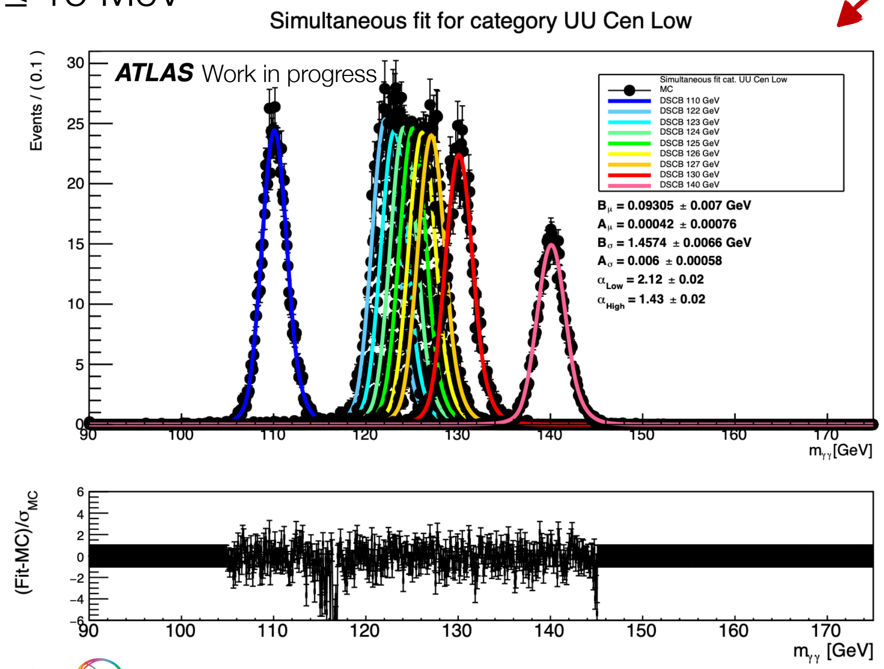

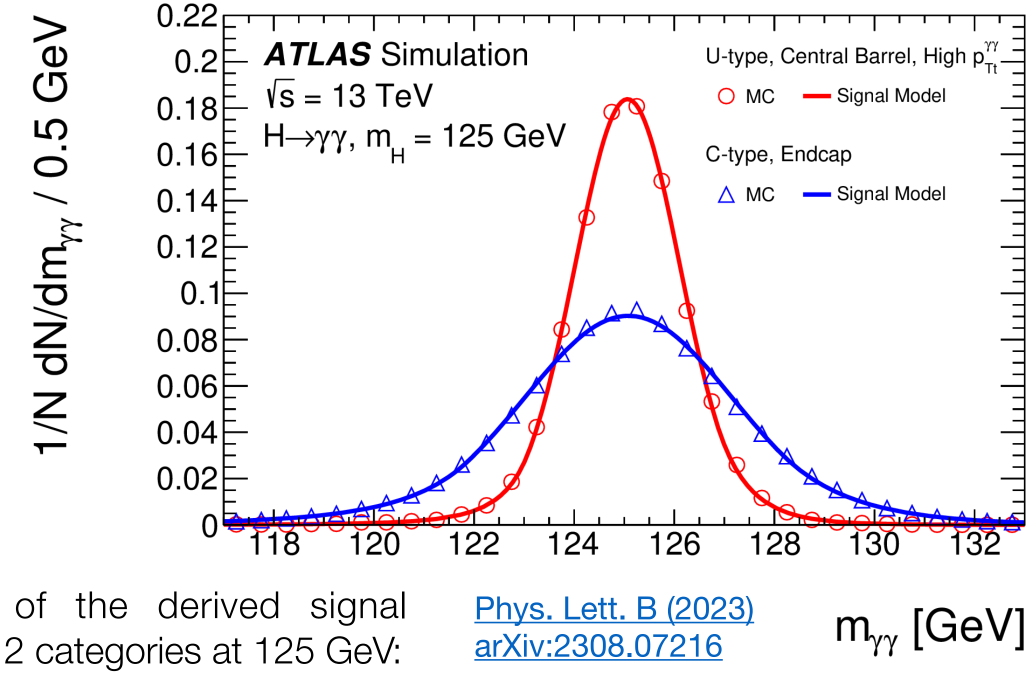

Example of the derived signal model for 2 categories at 125 GeV:

Phys. Lett. B (2023)
arXiv:2308.07216

3) $H \to \gamma\gamma$ Run 2: background model

The $\gamma\gamma$ QCD non-resonant bkg, $\gamma\gamma$ **irreducible** ($\sim 80\,\%$) + γ-jet + di-jet **reducible** ($\leq 20\,\%$), is modelled with analytical functions $\forall$ category and is almost **completely data-driven**

- the mass measurement is **not** very sensitive to bkg model

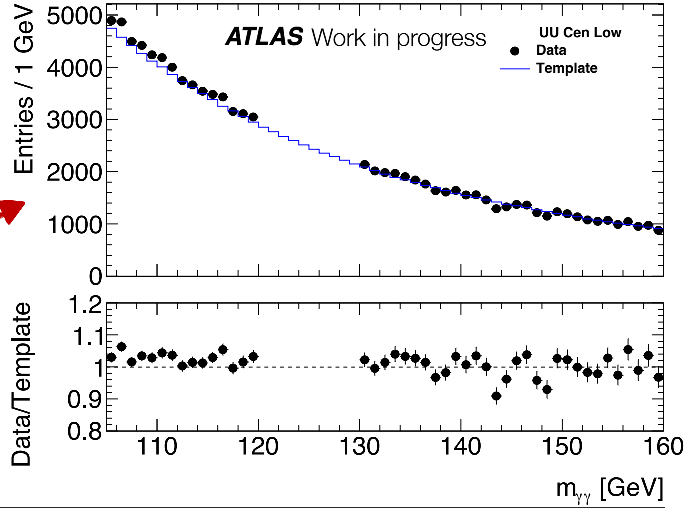

Strategy $\forall$ category:

1. Measure fractions of $\gamma\gamma$, γj and jj backgrounds with a 2xABCD method
2. Construct background-only templates starting from Sherpa $\gamma\gamma$ +reweighted $m_{\gamma\gamma}$ shapes from data-CR γj and jj
3. Perform **Spurious Signal test** to assign an **analytical function + systematic**: test a set of analytical functions (exp, power-law) and choose the one that minimizes the bias on a bkg-only template with the minimal number of d.o.f.
4. **Parameters and normalization** fitted on data sidebands in $m_{\gamma\gamma}$ ϵ [105, 160] GeV, blinding range $m_{\gamma\gamma}$ ϵ [120, 130] GeV, floating in the final fit

Background fit for category UU Cen Low

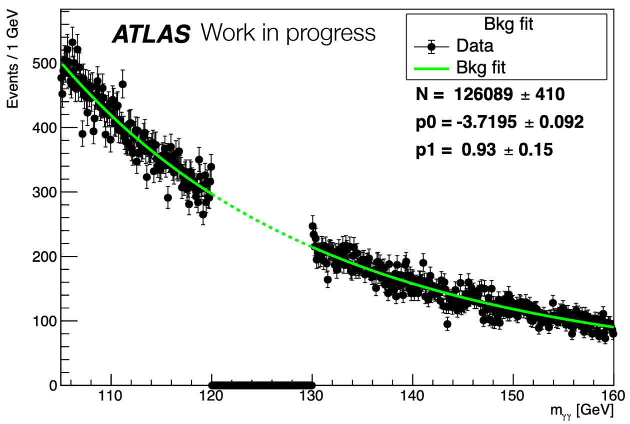

Category	m_H	n_S	Function	$p(\chi^2)$ %
UU Cen High	127.0	0.235	Exponential	27.1
UU Cen Med	123.0	5.31	Exponential	20.8
UU Cen Low	123.0	25	ExpPoly2	81.8
UU OutBarrel High	125.5	0.766	Pow	4.13
UU OutBarrel Med	126.0	4.92	ExpPoly2	53.1
UU OutBarrel Low	123.5	34.9	ExpPoly2	26.4
UU EndCap	123.0	63	ExpPoly2	15.6
Conv Cen High	126.5	-0.529	Pow	21.3
Conv Cen Med	123.5	6.99	Exponential	8.27
Conv Cen Low	124.5	21.2	ExpPoly2	40.5
Conv OutBarrel High	126.5	2.35	Exponential	12.8
Conv OutBarrel Med	126.5	6.97	ExpPoly2	69.1
Conv OutBarrel Low	125.5	28.7	ExpPoly2	59.4
Conv EndCap	126.5	137	ExpPoly2	1.53

4) $H \to \gamma\gamma$ Run 2: main experimental systematic uncertainties, PES

Main experimental systematic uncertainties are photon energy scale (**PES**) that affect μ_{CB}, $\forall$ category:

- Benefit from **excellent EGamma precision calibration recommendations**
- **Procedure**: auxiliary MC samples where the syst. variations ($\pm 1\sigma$) are applied upstream and their effect is propagated to the $m_{\gamma\gamma}$ distribution
- PES: 67 impacts computed as variation of the mean of the $m_{\gamma\gamma}$ distribution

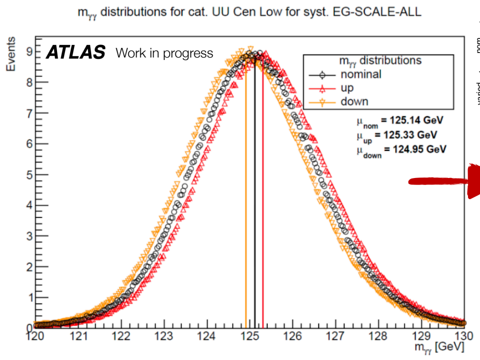

$\forall$ impact

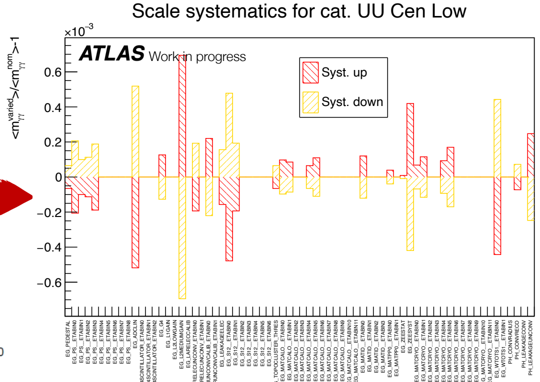

$\forall$ category

Additional reduction for PES comes from **EGamma linearity fit**:

- measurement of the residual p_T-dependent energy scale α' as a function of the nominal (p_T-dependent) PES systematics from $Z \to ee$ events in (p_T, η) bins

$$E_{\text{data}} = E_{\text{MC}}[1 + \alpha(\eta)(1 + \alpha'(|\eta|, p_T))]$$

$$\alpha' \propto \sum_{k}^{N_{sys}} \theta_k$$

- The new systematics are obtained by a Chi2 fit of the scale parametrization on the measured residual scale
- Output of the fit are constrained and correlated systematic uncertainties

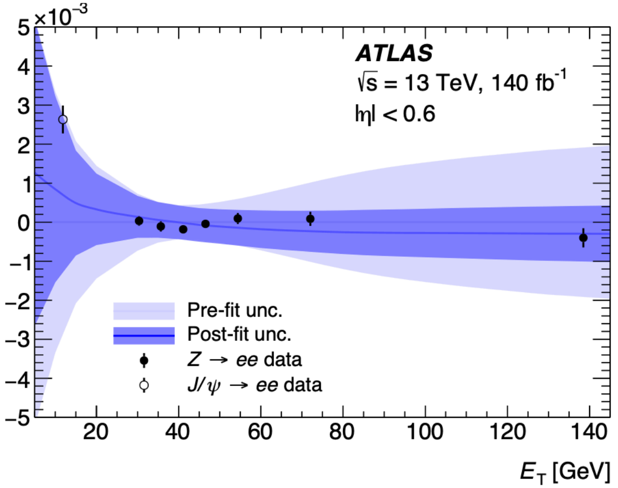

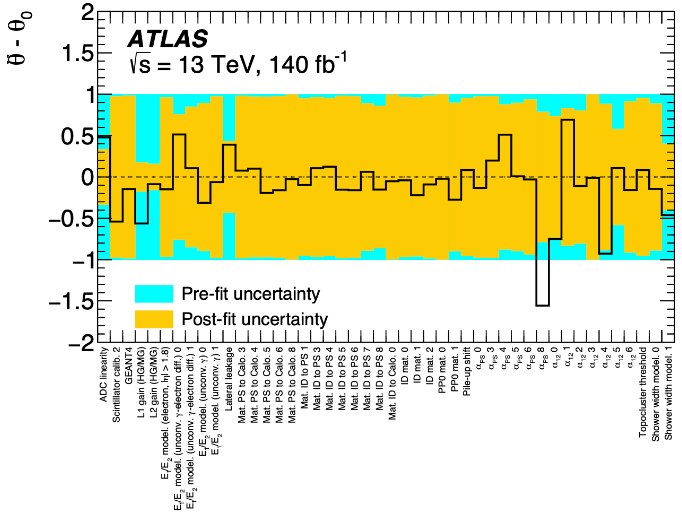

CERN-EP-2023-128

4) $H \rightarrow \gamma\gamma$ Run 2: main experimental systematic uncertainties, PES

The **EGamma linearity post-fit** information is propagated to the $\gamma\gamma$ mass analysis by

- applying the residual p_T-dependent energy scales per photon on **data** to obtain new $m_{\gamma\gamma}$ values
- modifying the NPs constraints in the **likelihood**, using a multidimensional Gaussian with the covariance matrix of the linearity fit, instead of single independent Gaussian constraints $$\prod_j G(0|\theta_j,1) \rightarrow G(0|\vec{\theta}, \sum n_{NP} x n_{NP})$$

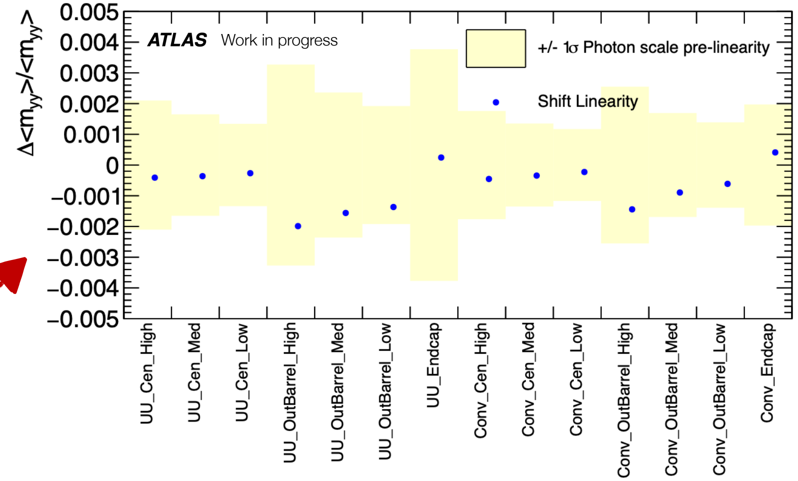

The **linearity** application in the mass analysis causes a **shift** on m_H that is **within the pre-linearity uncertainty** ∀ category

The **final reduction in PES** systematic uncertainties is close to a **factor 4** wrt previous [partial Run 2 analysis @ 36 ifb](#)!

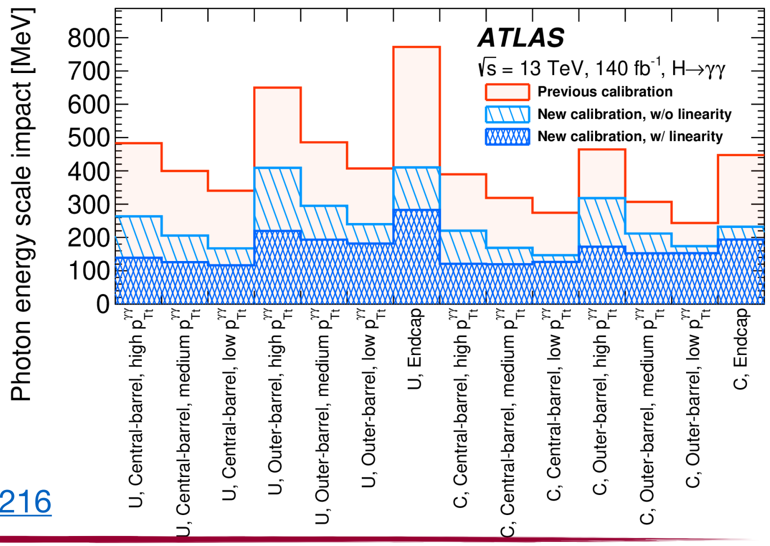

5) Secondary systematic uncertainties: other $\sim 10^2$ uncertainties are included in the model, backup slide 27

[Phys. Lett. B (2023) arXiv:2308.07216](#)

1) Event categorisation – Past categorisations

Event categorisation: selected events are divided in mutually exclusive categories optimised to reduce the total expected uncertainty on m_H. Regions with different:

- signal-to-bkg ratio $\frac{S}{B}$ and significance $Z \sim \frac{S}{\sqrt{B}}$
- invariant mass **resolution** (σ) of the $m_{\gamma\gamma}$ peak
- **systematic** uncertainties on photon energy scale (PES)

} γ kinematic variables as η, p_{Tt}, conversion status

Run1, 7/8 TeV, 25 fb^{-1} [Run1]

η:	Central	Rest	Trans
UU=2γUnconv	High / Low	High / Low	
Conv, ≥ 1γ Conv	High / Low	High / Low	

10 categories

- Central: both γ with |η|<0.75
- Trans: one γ with 1.3 < |η| < 1.75
- Rest: all the other events
- High/Low: events with $p_{Tt}^{\gamma\gamma} \gtrless 70$ GeV

Partial Run2, 13 TeV, 36 fb^{-1} [Run2@36ifb]

31 categories from STXS 2016 coupling analysis, 4% worst wrt to Run1 categorisation:

- 10 ggH categories, with ggH 0J split in CEN/FWD regions;
- 4 VBF categories;
- 8 categories for the associate production with a vector boson (W and Z);
- 9 categories for the associate production with a $t\bar{t}$ or single t

4) Main experimental systematic uncertainties: PES and PER

- Photon energy scale (**PES**) and photon energy resolution (**PER**) systematics affect μ_{CB} and σ_{CB}, ∀ category:
  - Procedure: auxiliary MC samples where the syst. variations ($\pm 1\sigma$) are applied upstream and their effect is propagated to the $m_{\gamma\gamma}$ distribution
  - PES: 67 NPs computed as variation of the mean of the $m_{\gamma\gamma}$ distribution $\boxed{\delta_{PES}(\pm 1\sigma) = \frac{\langle m_{\gamma\gamma}^{\pm 1\sigma} \rangle}{\langle m_{\gamma\gamma}^{nom} \rangle} - 1}$
  - PER: 9 NPs (grouped in 5 NPs to match Run1 scheme) as variation of the inter-quartile of the $m_{\gamma\gamma}$ distribution $\boxed{\delta_{PER}(\pm 1\sigma) = \frac{IQR^{\pm 1\sigma}}{IQR^{nom}} - 1}$

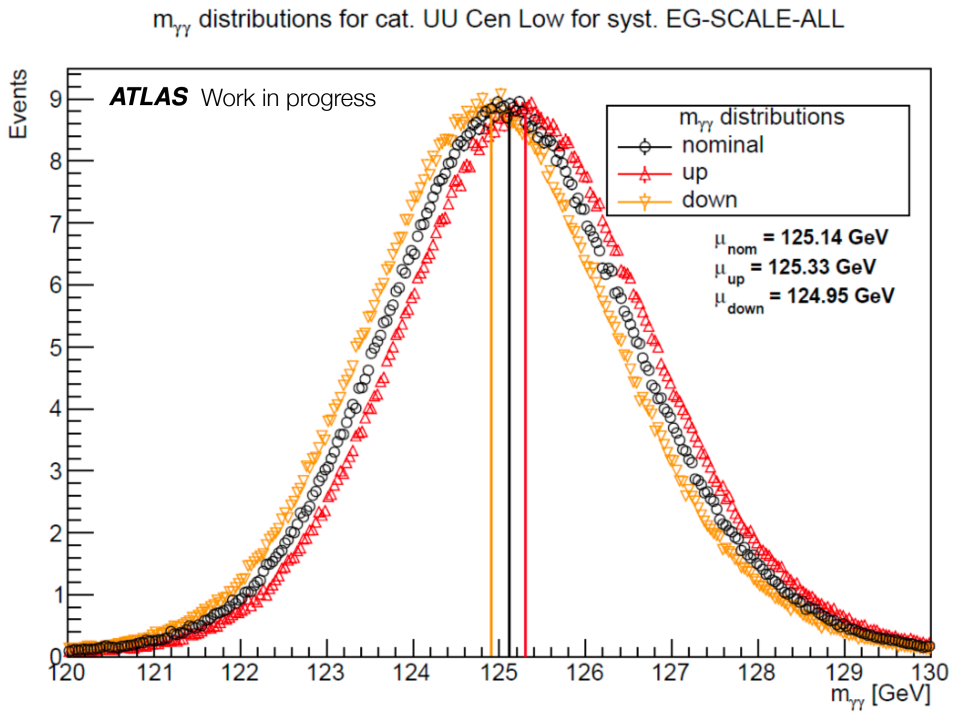

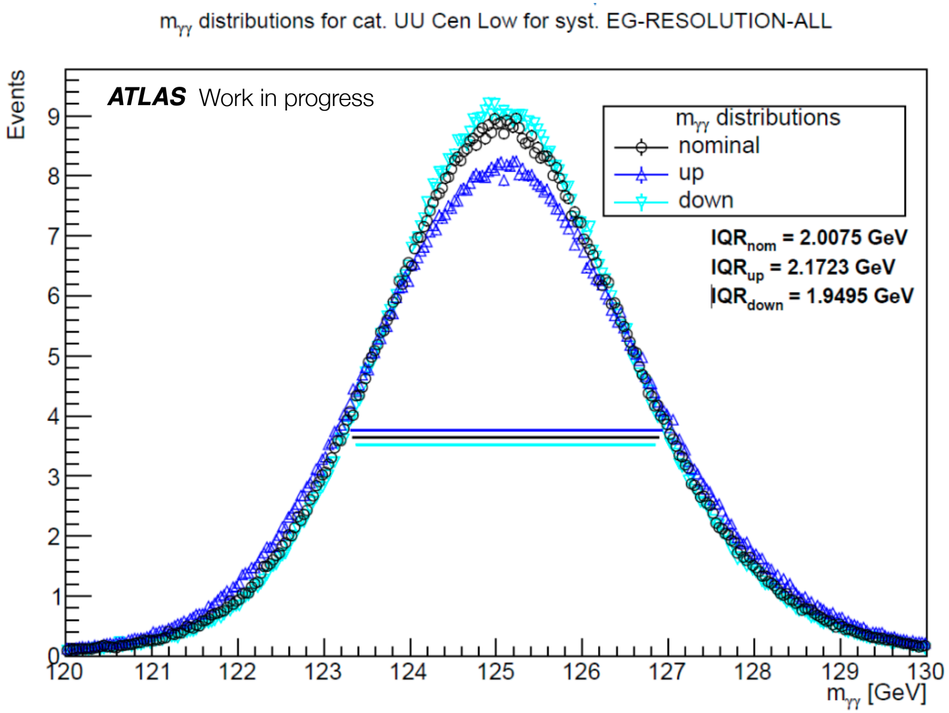

5) $H \to \gamma\gamma$ Run 2: secondary systematic uncertainties 📊

Additional and secondary systematic uncertainties are included in the likelihood model

- **Signal and background modelling**: an inaccurate model can cause a bias in the m_H measurement
  - Evaluated by injecting sig (bkg) MC sample over a bkg (sig) Asimov ∀ category, then refit with S+B model and compute m_H shift
  - Effect uncorrelated among categories, impact of **1 (14) MeV** for signal (background)
- **Interference** between $gg \to \gamma\gamma$ and $gg \to H \to \gamma\gamma$ processes causes a shift of the m_H
  - Evaluated by injecting interference MC sample over a S+B Asimov ∀ category, then refit with S+B model and compute m_H shift
  - Effect correlated among categories, expected **26 MeV** impact
- Photon energy **resolution** (PER): evaluated as interquartile difference of $m_{\gamma\gamma}$ distribution per category, applied on width of DSCB
- Photon **conversion reconstruction** affecting category migrations
  - Estimated with data/MC comparison in $Z \to ll\gamma$ events, correlated to corresponding scale effect
- **NN vertex selection** effect on m_H (5 MeV)
  - Estimated with data/MC comparison in $Z \to ee$ events where *e* are treated as unconverted photons
- Luminosity / BR $\gamma\gamma$ / QCD scale / PDF + α_s / Parton shower / Spurious signal / Yield
  - All included and with ~ null impact on m_H

5) Modelling systematics uncertainties

- **Signal modelling bias on m_H**: parameters of the signal model are fixed to the values obtained in the signal fit

  ⟶ an inaccurate signal model can cause a bias in the mass measurement

  - Fit dataset formed by signal (MC) and bkg (Asimov) with the analytical S+B model
  - Evaluate the bias as relative shift between the fitted and injected (125 GeV) m_H
  - Bootstrap to check the statistical significance

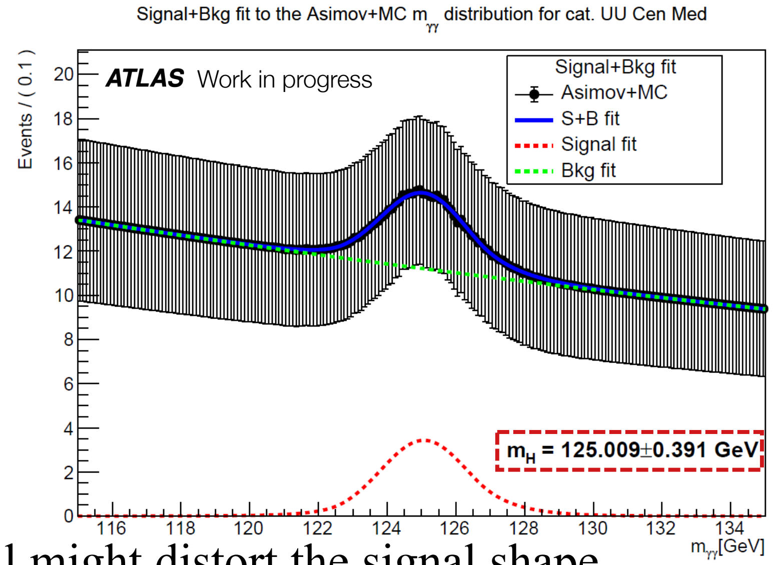

Similar procedure:

- **Background modelling bias on m_H:** dataset = signal (Asimov) + bkg (template)

- **Interference bias on m_H** : interference between $gg \rightarrow \gamma\gamma$ bkg and $gg \rightarrow H \rightarrow \gamma\gamma$ signal might distort the signal shape, the interference is **not** taken into account in the model ⟶ **neglecting** it can cause a bias in the mass measurement

Bias	Impact on m_H [MeV]
Signal	± 1
Background	± 14
Interference	± 26

fit on dataset = signal+bkg (Asimov) + interference (MC with $\Gamma_H^{SM} = 4.07$ MeV)

6) $H \to \gamma\gamma$ Run 2: expected and **observed** results 📊

- Checks with **different fit configurations**: ✅
  - Without linearity
  - Different μ configurations (1 global μ or $\mu_F+\mu_V$ or $\mu_{ggH} + \mu_{VBF} + \mu_{rest}$)
- **Internal compatibility studies**

Test 1: **general compatibility** of m_H in all the categories with global m_H value. Instead of only m_H, insert in our model $m_H + \Delta_{cat}$ $\forall$ category, 14 Δs

- Null hypothesis: *"mass is the same in each category"* $\to \forall \Delta_{cat} = 0$
- Alternative hypothesis 1: *"the values of m_H in all the cat. are different"* $\to$ Fit with all the 14 Δs free

$$q_0 = -2\log\frac{L(\Delta_1 = 0, \Delta_2 = 0, \ldots \Delta_n = 0, \hat{\hat{m}}_H)}{L(\hat{\Delta}_1, \hat{\Delta}_2, \ldots, \hat{\Delta}_n, \hat{m}_H)}$$

→ Global p-value = χ^2 distribution with 13 d.o.f. = **0.077**

Compatibility checks	Global p-value %
Test 1: **general compatibility** of m_H in all the categories with global m_H value	7.7
Test 2: compatibility of groups of categories: **conv vs. unconv**	48
Test 3: compatibility of groups of categories: **η** vs η regions (Central, OutBarrel, Endcap)	43
Test 4: compatibility of groups of categories: **pTt** vs pTt regions (High, Low, Med)	5.7
Test 5: compatibility of different **pileup** regions (using a pileup based categorisation, 5 categories)	43
Test 6: compatibility of different **years** (using a years based categorisation, 2015+2016 vs 2017 vs 2018)	31

all p-values > 5% ✅

Compatibility checks on unblinded data

Test 1: **general compatibility** of m_H in all the categories with global m_H value.
Instead of only m_H, insert in the ws $m_H + \delta_{cat}$ $\forall$ category, 14 δs

- Null hypothesis: *"mass is the same in each category"* $\rightarrow \forall \delta_{cat} = 0$

- Alternative hypothesis 1: *"the values of m_H in all the cat. are different"*

  Fit with all the 14 δs free

$$q_0 = -2\log \frac{L(\Delta_1 = 0, \Delta_2 = 0, \ldots \Delta_n = 0, \hat{\hat{m}}_H)}{L(\hat{\Delta}_1, \hat{\Delta}_2, \ldots, \hat{\Delta}_n, \hat{m}_H)}$$

  Global p-value = χ^2 distribution with 13 d.o.f. = **0.077**

- Alternative hypothesis 2: *"only m_H in category i is different"*

$$q_0^{(1)} = -2\log \frac{L(\Delta_1 = 0, \Delta_2 = 0, \ldots \Delta_n = 0, \hat{\hat{m}}_H)}{L(\hat{\Delta}_1, \Delta_2 = 0, \ldots, \Delta_n = 0, \hat{m}_H)}$$

  p-value of each δ for each category: compatibility of each category with global m_H, all > 0.05 except for UU Cen High

Category	p-value category
UU Cen High	0.01
UU Cen Med	0,11
UU Cen Low	0,29
UU OutBarrel High	0,66
UU OutBarrel Med	0,18
UU OutBarrel Low	0,36
UU EndCap	0,07
Conv Cen High	0,41
Conv Cen Med	0,71
Conv Cen Low	0,38
Conv OutBarrel High	0,10
Conv OutBarrel Med	0,70
Conv OutBarrel Low	0,61
Conv EndCap	0,99

Compatibility checks on unblinded data

Test 1: **general compatibility** of m_H in all the categories with global m_H value.
Instead of only m_H, insert in the ws $m_H + \delta_{cat}$ $\forall$ category, 14 δs

Obtained with all δs free, alternative hypothesis 1

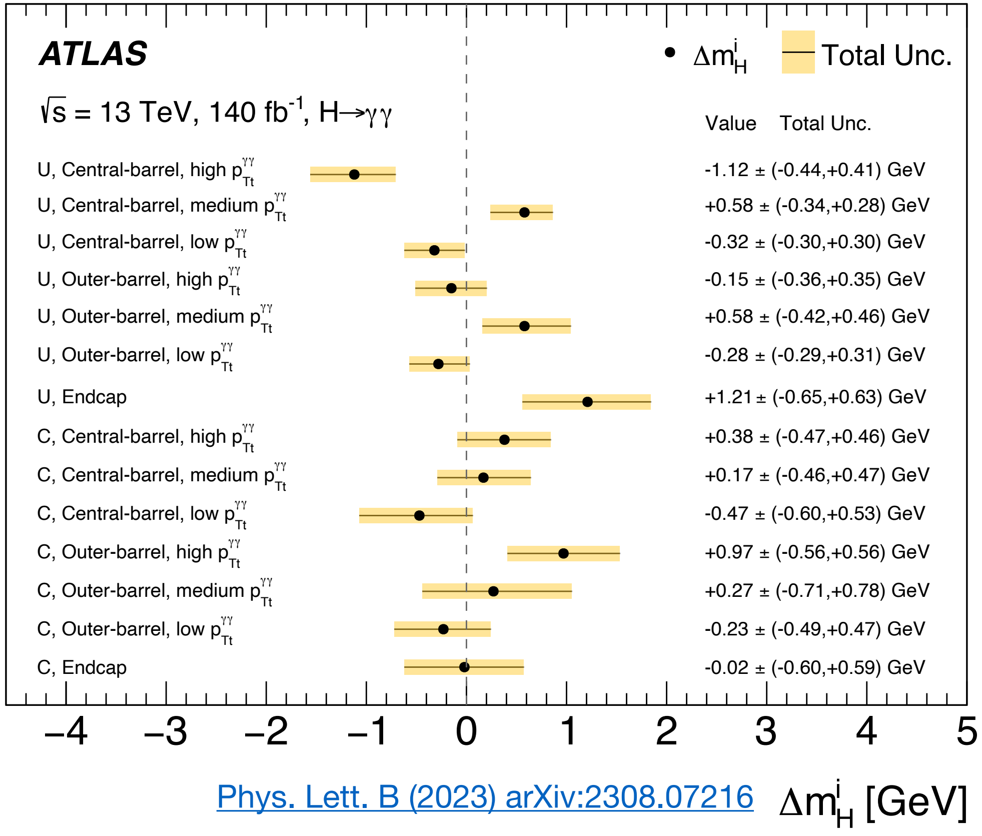

Phys. Lett. B (2023) arXiv:2308.07216

Obtained with 1 δ free at a time

Category	**p-value category**
UU Cen High	0.01
UU Cen Med	0,11
UU Cen Low	0,29
UU OutBarrel High	0,66
UU OutBarrel Med	0,18
UU OutBarrel Low	0,36
UU EndCap	0,07
Conv Cen High	0,41
Conv Cen Med	0,71
Conv Cen Low	0,38
Conv OutBarrel High	0,10
Conv OutBarrel Med	0,70
Conv OutBarrel Low	0,61
Conv EndCap	0,99

Higgs boson Run2 mass measurement H → γγ: systematic uncertainties

Experimental systematic uncertainties: the **energy calibration procedure** on the photons has an impact on m_H measurement

- **LAr cell non-linearity**: non-linearity of Layer2 gain cell energy measurement and to the uncertainty on the intercalibration between the different readout gains

- **Layer calibration**: accounts for the impact of the Layer1 and Layer2 (EM calorimeter) intercalibration on the reconstructed particle energy. The scale factors $\alpha_{1/2}$ used to intercalibrate the first two layers of the electromagnetic calorimeter are evaluated as a function of $|\eta|$ and E_T

- **Material**: the Inner Detector, the cryostat and calorimeter material uncertainties are obtained by comparing the energy response in Monte Carlo samples simulated with nominal and modified detector geometry. The difference in the energy response are scaled comparing the material variation of the corresponding distorted simulated sample with the actual material measurement uncertainties, yielding to the energy scale uncertainties

- **$Z \to e^+e^-$ calibration:** Z-based calibration fixes the energy scale and its uncertainty for electrons with transverse energy close to the average of those produced in Z decays ($p_T \sim$ 40 GeV). Photons produced in $H \to \gamma\gamma$ decay have a harder p_T spectrum so the uncertainties have to be extrapolated and the impact is generally larger

e/gamma calibration in Run 2

$\boxed{e/\gamma}$

Calibration workflow

CERN-EP-2023-128

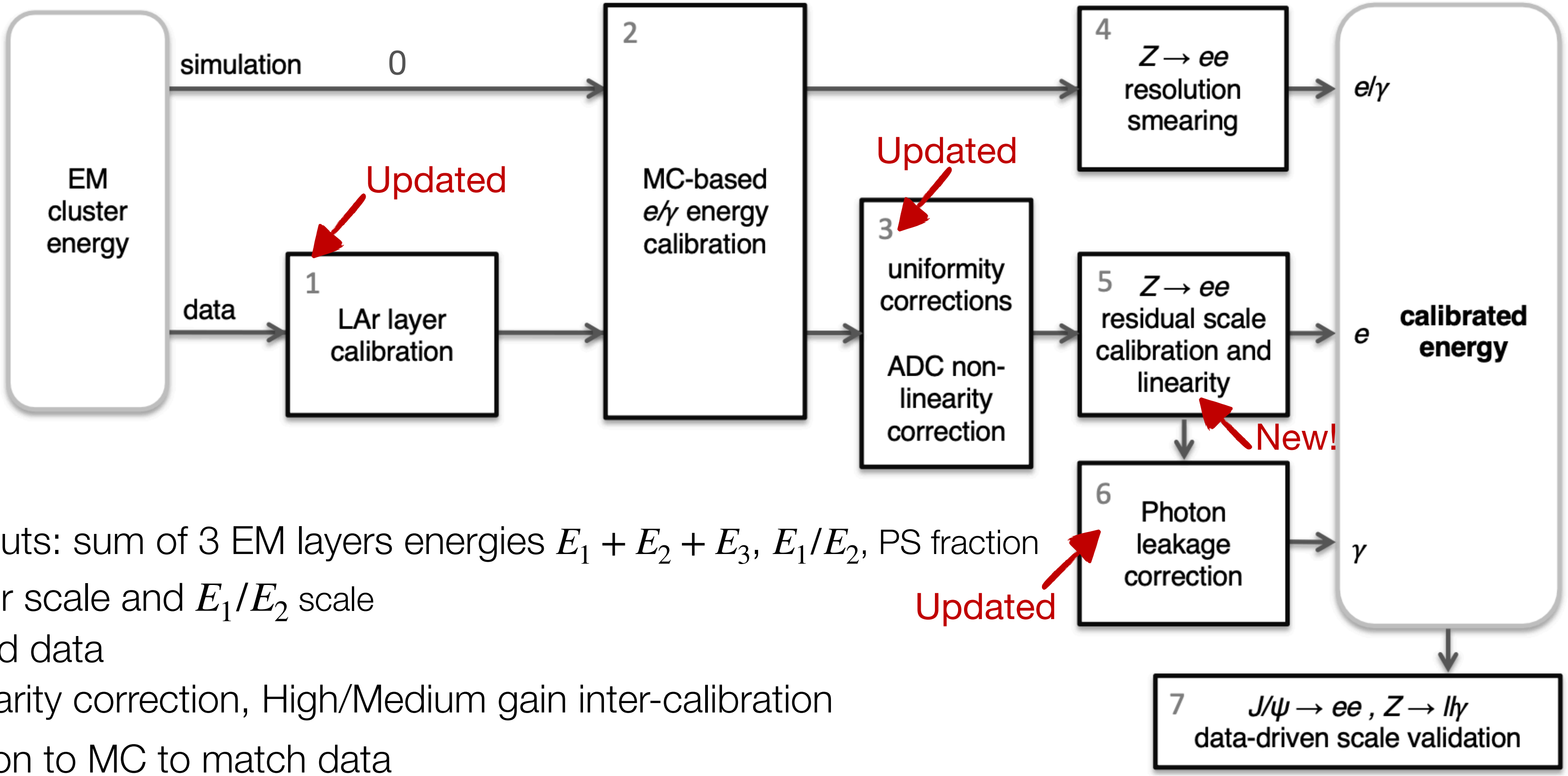

7 steps:

0. MVA calibration trained on MC. BDT inputs: sum of 3 EM layers energies $E_1 + E_2 + E_3$, E_1/E_2, PS fraction
1. **LAr layer inter-calibration**: presampler scale and E_1/E_2 scale
2. Application of MVA calibration to MC and data
3. **Uniformity corrections**: ADC non-linearity correction, High/Medium gain inter-calibration
4. $Z \to ee$ scale: apply resolution correction to MC to match data
5. $Z \to ee$ **scale**: apply scale correction to data to match MC + **new linearity fit**
6. **Photon leakage correction**
7. Validation of calibration chain with J/ψ and radiative Z

5. $Z \to ee$ scale and linearity fit

- A final adjustment of the calorimeter response is derived from samples of $Z \to ee$ events, so that the peak of the Z resonance reconstructed in data coincides with that in the simulation:
  - **Scale** corrections are applied to the data to match MC
  - **Resolution** corrections are applied to the MC to match data

Scale: $\boxed{E^{data} = E^{MC}(1 + \alpha(\eta))}$

Assumption: scales do not depend on $p_T \Rightarrow$ measure scales inclusively in p_T

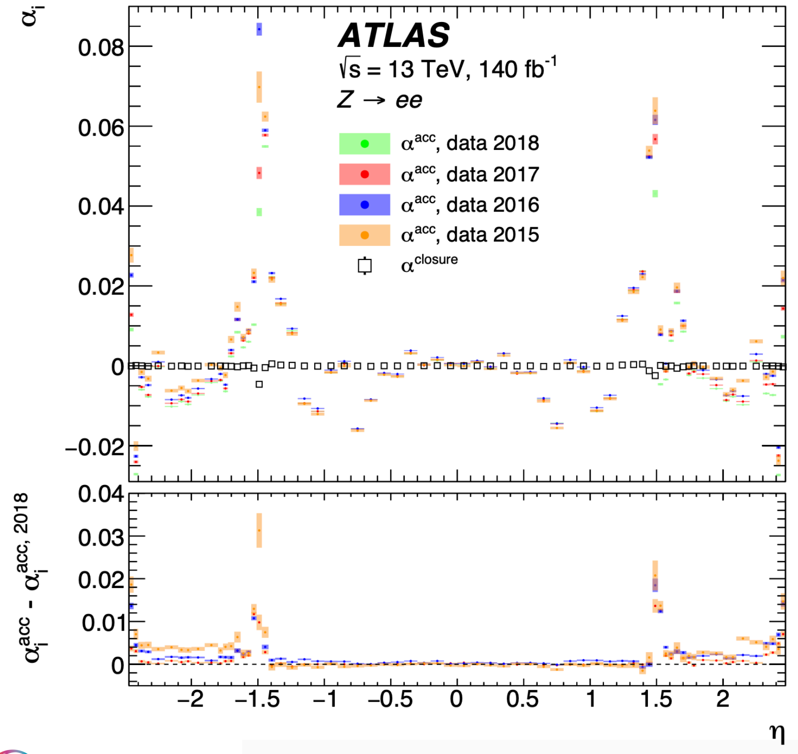

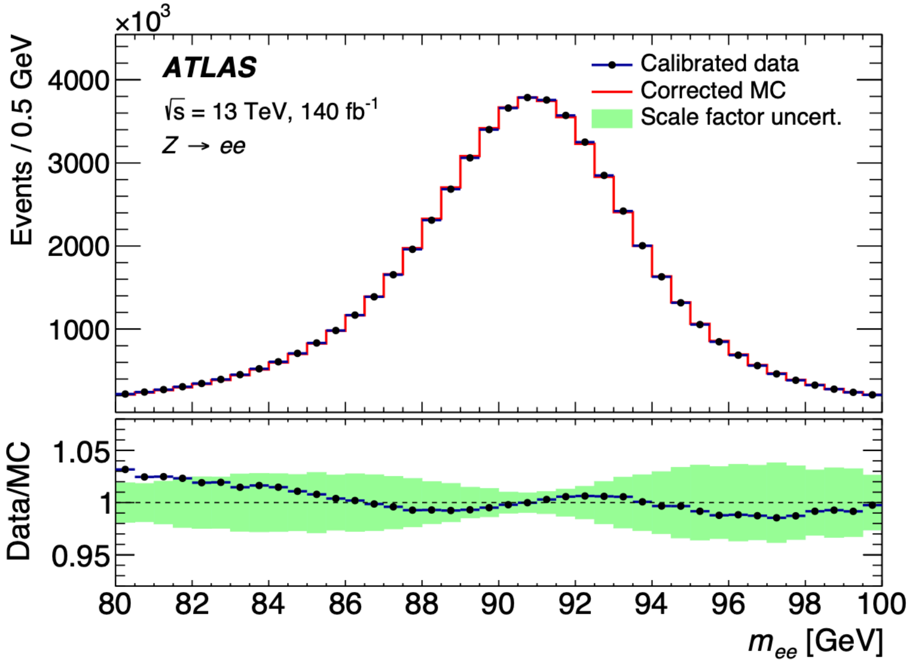

5. $Z \to ee$ scale and linearity fit

- A final adjustment of the calorimeter response is derived from samples of $Z \to ee$ events, so that the peak of the Z resonance reconstructed in data coincides with that in the simulation:
  - **Scale** corrections are applied to the data to match MC
  - **Resolution** corrections are applied to the MC to match data

Scale: $\boxed{E^{data} = E^{MC}(1 + \alpha(\eta))}$ → $\boxed{E^{data} = E^{MC}[(1 + \alpha(\eta))(1 + \alpha'(|\eta|, p_T))]}$ where $\alpha'(|\eta|, p_T|\theta) = \sum_k^{N_{sys}} \delta\alpha_k(\eta, p_T)\theta_k$

New linearity fit!

Measurement of the residual p_T-dependent energy scale α' as a function of the nominal (p_T-dependent) PES systematics θ_k from $Z \to ee$ events in (p_T, η) bins. Relax the assumptions that scales do not depend on E_T

5. $Z \rightarrow ee$ scale and linearity fit

- A final adjustment of the calorimeter response is derived from samples of $Z \rightarrow ee$ events, so that the peak of the Z resonance reconstructed in data coincides with that in the simulation:
  - **Scale** corrections are applied to the data to match MC
  - **Resolution** corrections are applied to the MC to match data

Scale: $\boxed{E^{data} = E^{MC}(1+\alpha(\eta))}$ → $\boxed{E^{data} = E^{MC}[(1+\alpha(\eta))(1+\alpha'(|\eta|, p_T))]}$ where $\alpha'(|\eta|, p_T|\theta) = \sum_k^{N_{sys}} \delta\alpha_k(\eta, p_T)\theta_k$

New linearity fit!

Fit output: pulled, constrained and correlated systematic uncertainties

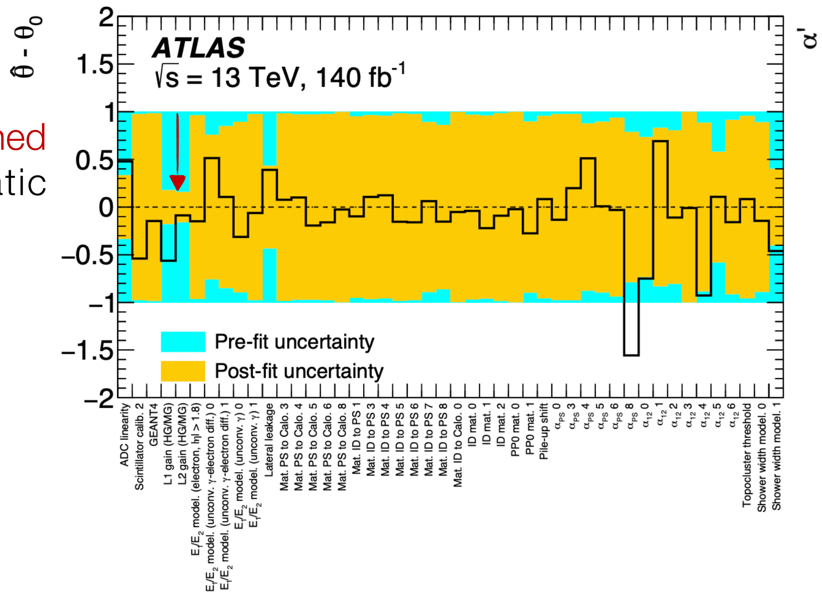

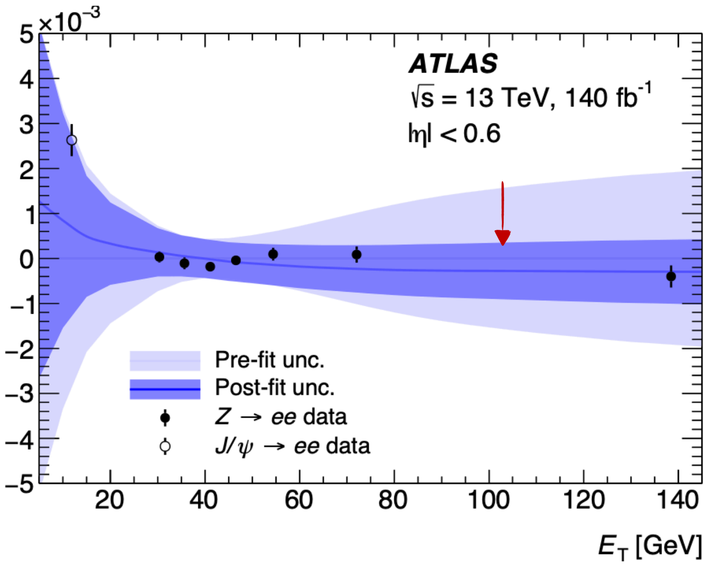

NP pulls give new prediction of **energy scale** (line), with **new uncertainties** accounting for constraints and correlations (dark band)

~ 50% (30%) constraint in **barrel (endcap)** for electron **@ 60 GeV**

1. LAr layer inter-calibration

- <u>Why it's needed</u>: the 4 longitudinal layers of the EM calorimeter (PS, L1, L2, L3) should be calibrated separately to provide a correct description of the calorimeter response as a function of E_T

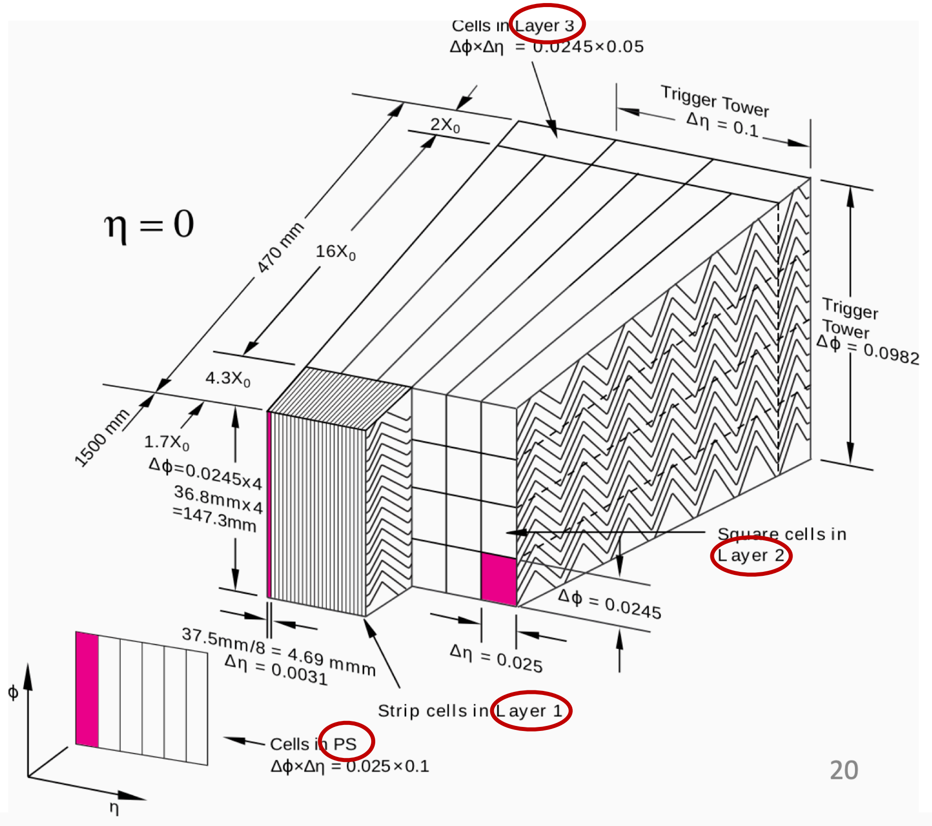

1. LAr layer inter-calibration

- Why it's needed: the 4 longitudinal layers of the EM calorimeter (PS, L1, L2, L3) should be calibrated separately to provide a correct description of the calorimeter response as a function of E_T

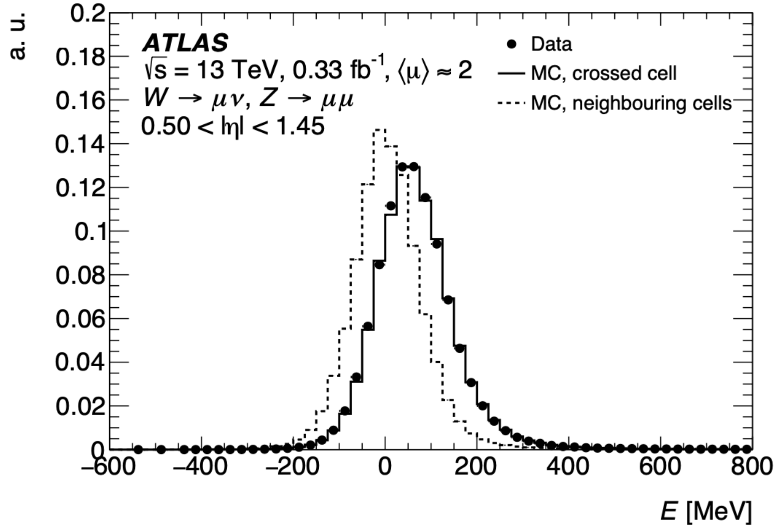

Presampler scale

- Presampler energy calibrated by scale factor $\boxed{\alpha_{\mathrm{PS}}(\eta) = \dfrac{< E_{\mathrm{PS}}^{data}(\eta) >}{< E_{\mathrm{PS}}^{MC}(\eta) >}}$
- Past: from e/γ samples
- **Now**: using μ from low pile-up data ($< \mu > \sim 2$): since muons are insensitive to material upstream the PS, effective way to measure direct response to PS, decorrelating the $\alpha_{\mathrm{PS}}(\eta)$ unc. from the unc. on the material in front of the PS
- Low noise thanks to low pile-up
- Evaluated in 9 $|\eta|$ PS bins
- Bias up to **5%** with uncertainty **2-4%**

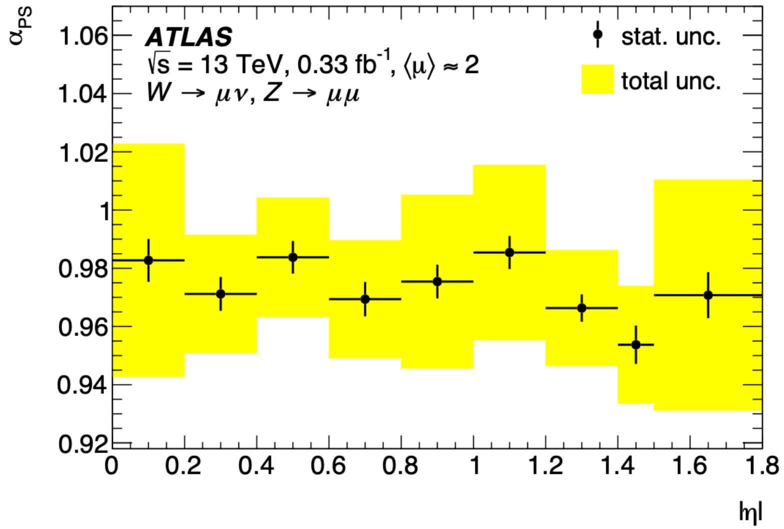

1. LAr layer inter-calibration

- Why it's needed: the 4 longitudinal layers of the EM calorimeter (PS, L1, L2, L3) should be calibrated separately to provide a correct description of the calorimeter response as a function of E_T

E_1/E_2 scale

- The ratio of E_1/E_2 is calibrated by scale factor

$$\boxed{\alpha_{1/2} = \frac{< E_1^{data} > / < E_2^{data} >}{< E_1^{MC} > / < E_2^{MC} >}}$$

- Past: only with μ

- **Now**:

calibration with μ:
- Most Probable Value method
- Truncated Mean method

calibration with e:
- E/p distribution
- m_{ee} distribution

- Good agreement between the 4 single results

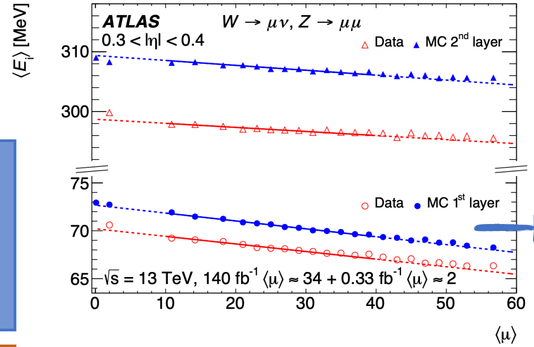

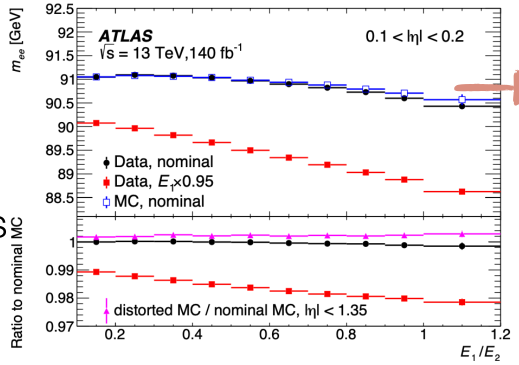

combined μ at pile-up ~ 0

combined e

Combined e/μ

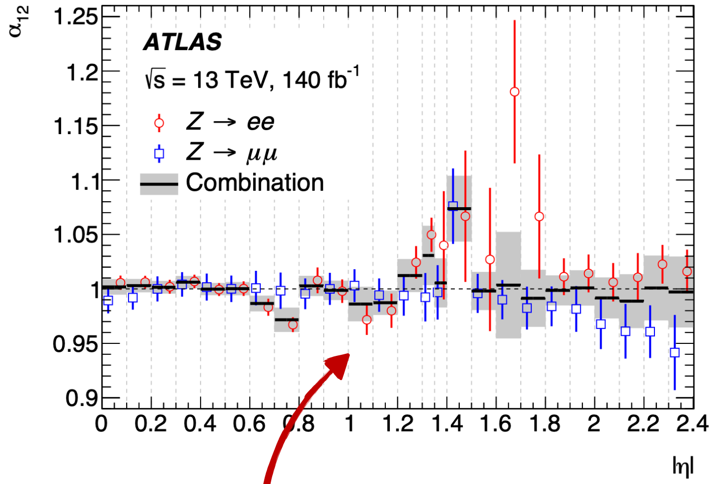

- Uncertainty up to **0.6%** (**3%**) in central barrel (endcap)
- **Gain a factor 2 improvement on barrel uncertainty**

3. Uniformity corrections

- Why it's needed: additional corrections applied to data to account for **response variations** not included in the simulation in specific detector regions, e.g. regions with **non-optimal high voltage**, **azimuthal** non-uniformities, or biases associated with the liquid-argon calorimeter's **electronics calibration**.

3. Uniformity corrections

- Why it's needed: additional corrections applied to data to account for **response variations** not included in the simulation in specific detector regions, e.g. regions with **non-optimal high voltage**, **azimuthal** non-uniformities, or biases associated with the liquid-argon calorimeter's **electronics calibration**.

ADC non-linearity

- Cell energy reconstruction: digitized **ADC counts** are converted to **current** using 3 linear gains (HG, MG, LG). Current → cell energy
- The conversion between ADC counts and current is assumed **linear** and is calibrated during dedicated electronic calibration runs with known injected current
- Non-zero residuals, caused by intrinsic non-linear behaviour of the electronics
- New: **now fitting also the residuals** between linear fit and measurements, ∀ cell

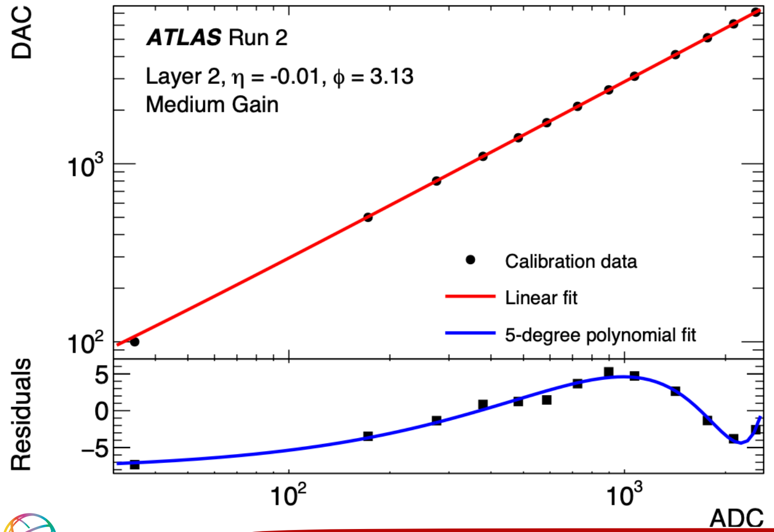

Energy correction

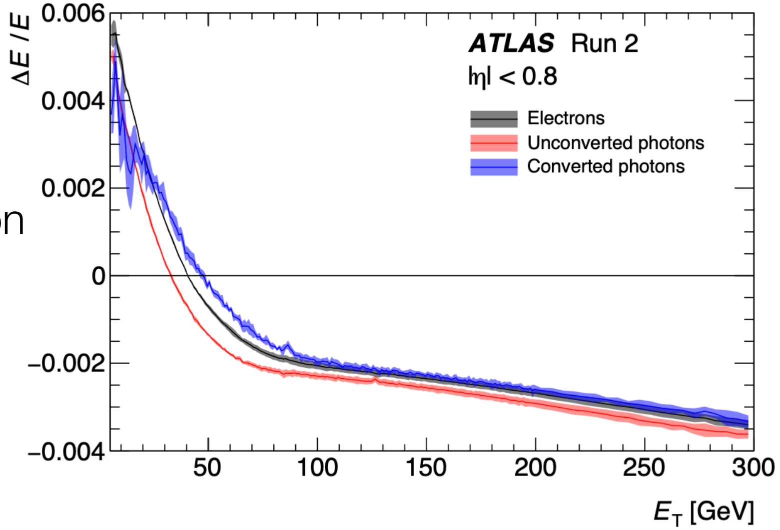

3. Uniformity corrections

- <u>Why it's needed</u>: additional corrections applied to data to account for **response variations** not included in the simulation in specific detector regions, e.g. regions with **non-optimal high voltage**, **azimuthal** non-uniformities, or biases associated with the liquid-argon calorimeter's **electronics calibration**.

High/Medium gain intercalibration

- 3 gains (HG, MG, LG) used to digitize the signal
- **Different gains** are used **depending on recorded cell energy**: cells from Z→*ee* mostly in HG. At higher energy (H→γγ) HG and MG are both important → needed HG/MG intercalibration
- How: using **special runs** with different thresholds, to have more MG with Z→*ee*. Comparing Zee mass peak between special and standard runs
- Effect reduced by **factor 2** thanks to new ADC correction (slide 8)
- Reduction also in the uncertainty

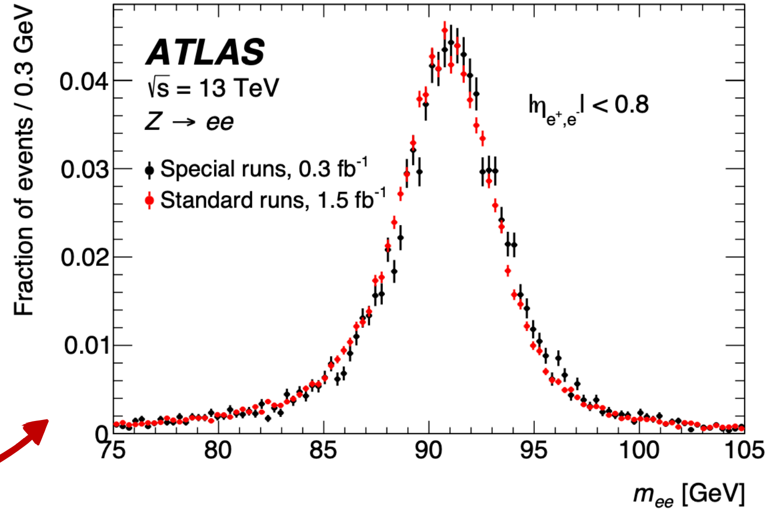

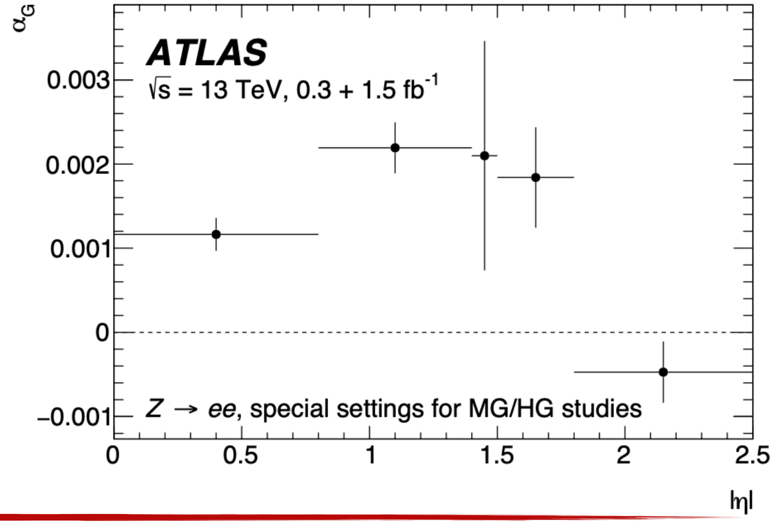

6. Lateral leakage correction

- Why it's needed:
  - e and γ deposit 1%-6% of their E outside of the cluster used in the reconstruction, depending on E_{T}, η and the particle type
    → bias in the reconstructed E could appear in data if this lateral leakage is mis-modelled by the simulation
  - Photon-specific corrections are needed to account for differences in the lateral development of e and γ showers
- **Lateral leakage** $l = \frac{E^{L2}_{7\mathrm{x}11}}{E^{L2}_{\mathrm{nom}}} - 1$, where nom = 3x7 cells
- Evaluate data - MC difference for each particle type

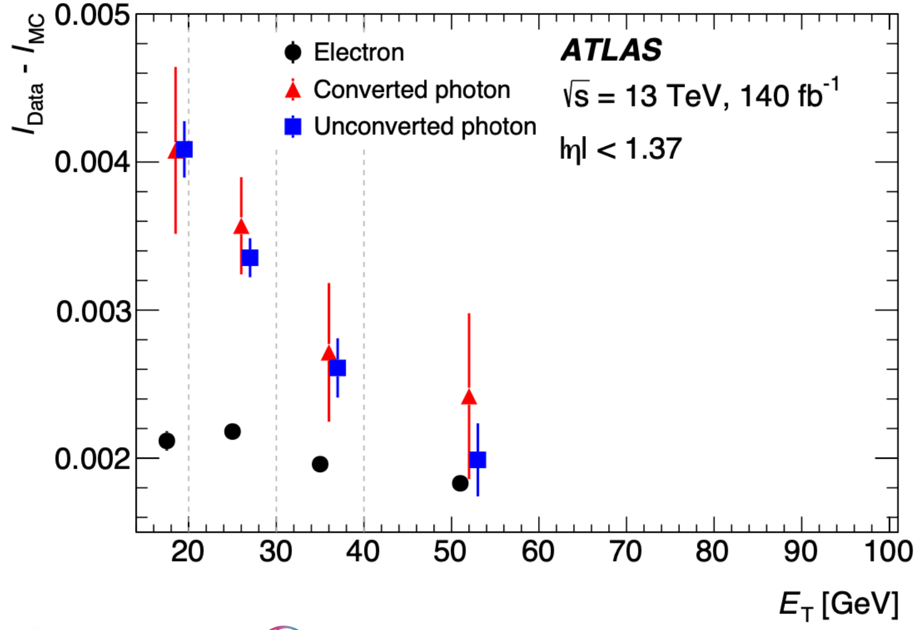

- Observations:
  - **Electron** leakage mismodelling nearly flat in E_T, absorbed by Zee
  - **Photons** are worse at low E_T: **correction to photon energy scale** from double difference between electrons and photons in data and simulation $\alpha_l = (l_e - l_\gamma)^{data} - (l_e - l_\gamma)^{MC}$
    - **new**, before only considered as a systematic uncertainty

Systematic unc. reduced by a **factor 2**

Muon calibration in Run 2

$\boxed{\mu}$

Calibration workflow

arXiv:2212.07338

Muons are reconstructed using information from the ID and/or MS sub-detectors, which provide two independent measurements.

Definitions of muon candidates:

- **ID** tracks: reconstructed using ID hits only
- **SA** (Standalone tracks): obtained using MS hits only
- **CB** (Combined tracks): obtained by starting from a MS track and matching it to an ID track

μ momentum calibration chain:

- **Charge-dependent sagitta bias** scale correction $\leftarrow$ new methodology
- Charge independent scale/resolution correction
- Validation

What's new:

- **Charge-dependent sagitta bias** scale correction $\leftarrow$ new methodology
- Inclusion of $J/\psi \to \mu\mu$ in scale/reso correction
- Dedicated calibration of **CB tracks** (before only done separately for ID and SA; CB obtained as average of the ID & MS contribution)

Charge dependent correction - Sagitta Bias

Why it's needed: residual misalignments introduce a **charge-dependent bias** in the momentum measurement

- Using $Z \to \mu\mu$ samples
- $\frac{q}{\hat{p}} = \frac{q}{p} + q\delta_S$ $\rightarrow$ $m^2_{\mu\mu} = \hat{m}^2_{\mu\mu}(1 + \delta_s(\eta, \phi)p_T^+ - \delta_s(\eta, \phi)p_T^-)$

  p $(\hat{p})$ is the corrected (uncorrected) momentum;

  δ_s = sagitta bias

The sagitta bias causes a bias in the invariant mass $\rightarrow$ broadening of the **resolution**

- Iterative process to determine the bias both in data and MC:

  1. $\delta_s(\eta, \phi)$ evaluation by minimising the variance of the $Z\mu\mu$ invariant mass distributions;
  2. Correct $\hat{p}_T \to p_T$
  3. New p_T values are used to recalculate the invariant mass distribution

Charge dependent correction - Sagitta Bias

Why it's needed: residual misalignments introduce a **charge-dependent bias** in the momentum measurement

- **Correct data** with bias not modelled by MC: $\delta_s(\eta,\phi) = \delta_s^{data}(\eta,\phi) - \delta_s^{MC}(\eta,\phi)$
- Dedicated correction for CB, ID, and MS muons
- Biases are reduced to less than $2 \cdot 10^{-4}$ TeV $^{-1}$ in all regions of the detector, $\sim$ 2 orders of magnitude improvement
- **Resolution improvement** on the $Z \rightarrow \mu\mu$ peak

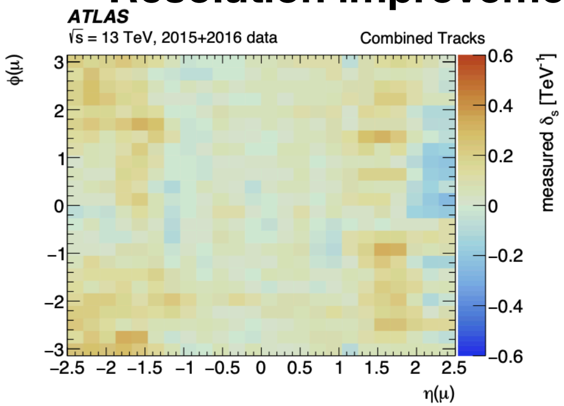

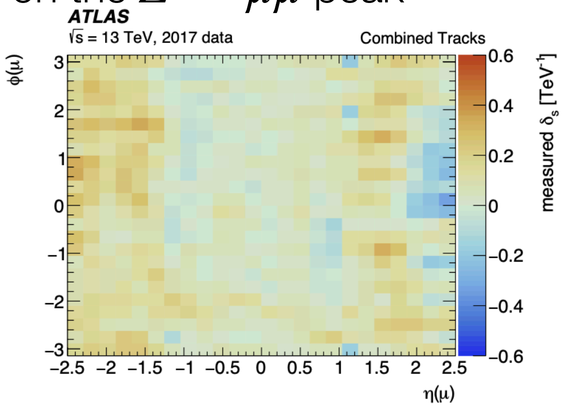

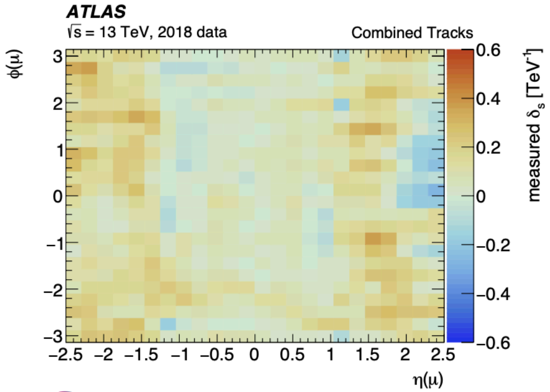

Before correction → After correction

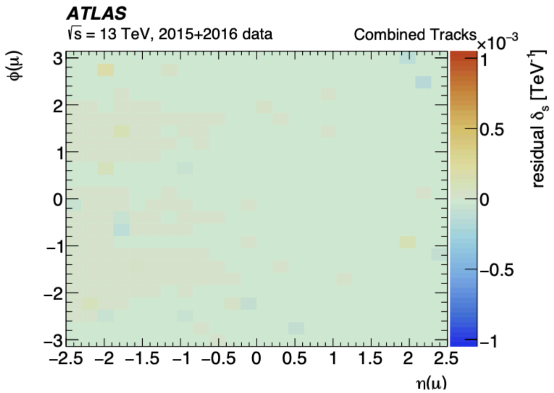

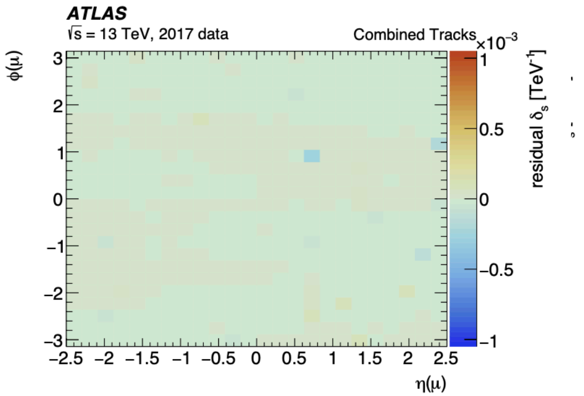

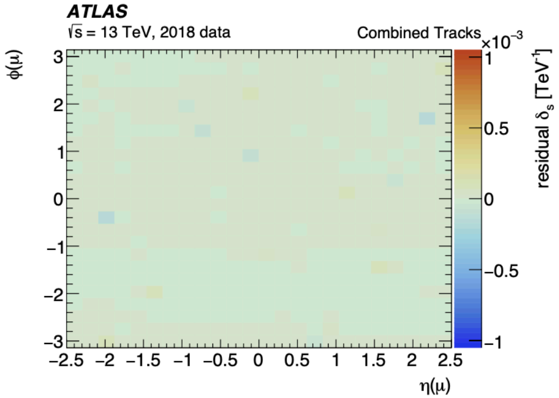

Scale and resolution corrections

Muon momentum calibration **applied to simulated events**, to improve the agreement between the simulation and the data.

- Using $Z \to \mu\mu$ and $J/\psi \to \mu\mu$ data and simulation samples

Corrected p_T in MC

Uncorrected p_T in MC

Scale correction

$$p_{\mathrm{T}}^{\mathrm{Cor,Det}} = \frac{p_{\mathrm{T}}^{\mathrm{MC,Det}} + \boxed{\sum_{n=0}^{1} s_n^{\mathrm{Det}}(\eta,\phi)\left(p_{\mathrm{T}}^{\mathrm{MC,Det}}\right)^n}}{1 + \boxed{\sum_{m=0}^{2} \Delta r_m^{\mathrm{Det}}(\eta,\phi)\left(p_{\mathrm{T}}^{\mathrm{MC,Det}}\right)^{m-1} g_m}}$$

Resolution correction

- Determination of the $s_n(\eta,\phi)$ and $\Delta_r(\eta,\phi)$ corrections through a **fitting procedure**, comparing the invariant mass distributions for $Z \to \mu\mu$ and $J/\psi \to \mu\mu$ candidates in data and simulation
- Dedicated correction for **CB**, ID, and MS muons

New!

Example for CB muons:

Region	$\Delta r_1^{\mathrm{CB}} (\times 10^{-3})$	Δr_2^{CB} [TeV $^{-1}$]	s_0^{CB} [MeV]	$s_1^{\mathrm{CB}} (\times 10^{-3})$
$\lvert\eta\rvert < 1.05$ (large)	$6.7^{+1.4}_{-0.9}$	$0.08^{+0.04}_{-0.05}$	$-5.0^{+2.9}_{-4.0}$	$0.35^{+0.24}_{-0.22}$
$\lvert\eta\rvert < 1.05$ (small)	$6.5^{+1.3}_{-1.0}$	$0.11^{+0.05}_{-0.05}$	$-0.9^{+2.5}_{-3.6}$	$-0.83^{+0.25}_{-0.14}$
$1.05 \leq \lvert\eta\rvert < 2.0$ (large)	$10.3^{+2.6}_{-2.7}$	$0.24^{+0.10}_{-0.07}$	$-2.0^{+5.7}_{-6.7}$	$-0.83^{+0.39}_{-0.30}$
$1.05 \leq \lvert\eta\rvert < 2.0$ (small)	$8.9^{+1.7}_{-2.7}$	$0.29^{+0.08}_{-0.03}$	$-3.0^{+3.3}_{-4.0}$	$-0.80^{+0.26}_{-0.21}$
$\lvert\eta\rvert \geq 2.0$ (large)	$10.6^{+2.2}_{-2.7}$	$0.21^{+0.10}_{-0.07}$	$2.3^{+13}_{-9.3}$	$0.80^{+1.09}_{-0.42}$
$\lvert\eta\rvert \geq 2.0$ (small)	$11.5^{+2.2}_{-2.1}$	$0.26^{+0.08}_{-0.06}$	$-12.6^{+8.2}_{-9.7}$	$1.59^{+0.47}_{-0.43}$

Validation and performance

$J/\psi \to \mu\mu$, $Z \to \mu\mu$, $\Upsilon \to \mu\mu$ (fully independent) samples are used to **validate** the momentum corrections and measure the μ momentum reconstruction **performance**.

After MC correction for CB muons:

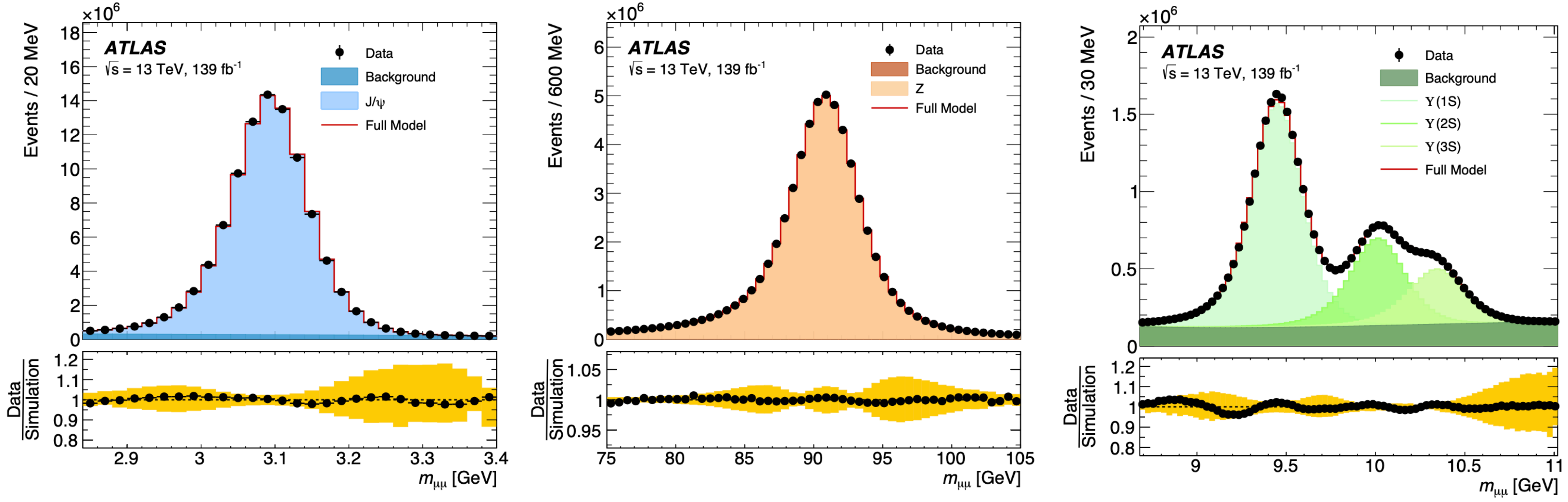

Validation and performance

$J/\psi \to \mu\mu$, $Z \to \mu\mu$, $\Upsilon \to \mu\mu$ (fully independent) samples are used to **validate** the momentum corrections and measure the μ momentum reconstruction **performance**.

p_T resolution obtained from simulation after application of all correction constants

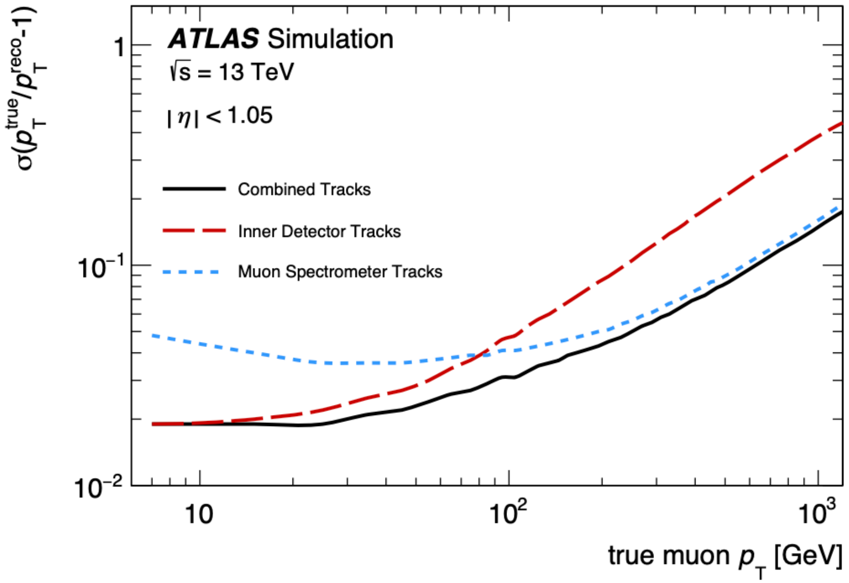

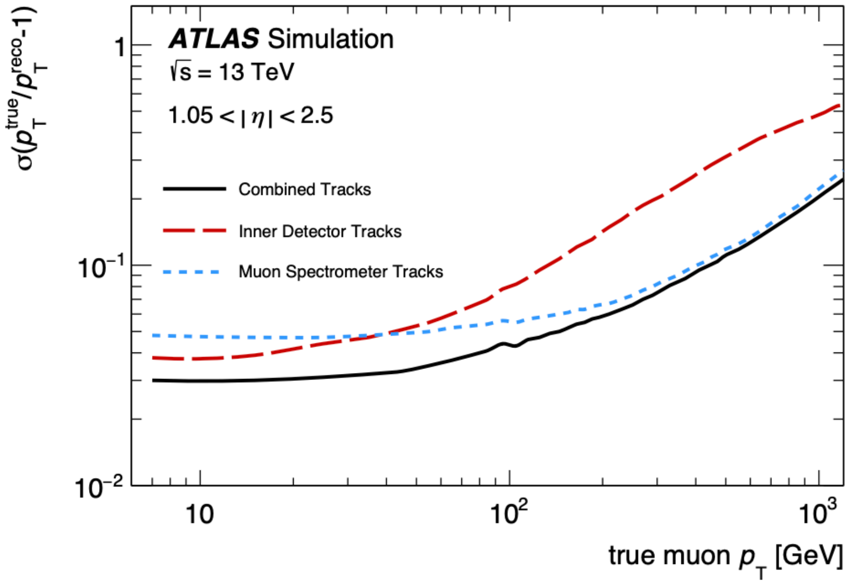

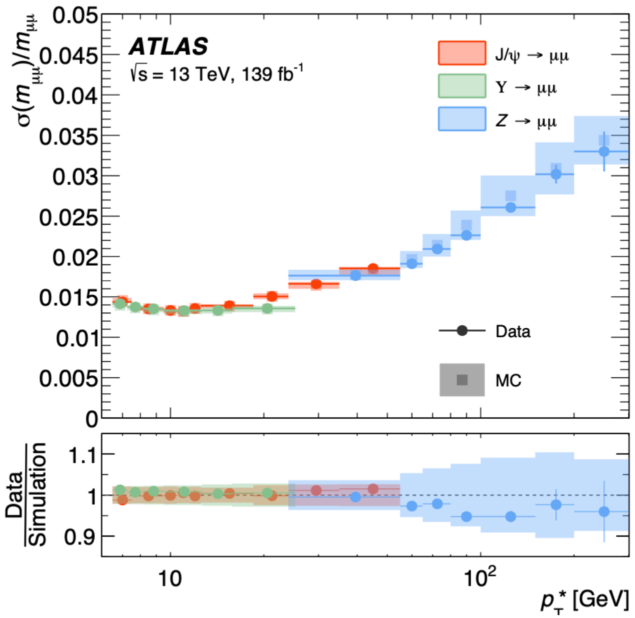

Di-muon invariant mass resolution obtained from simulation after correction

Systematics on scale parameters evaluation: $J/\psi \Longleftrightarrow$ Z extrapolation, FSR modelling, mass range, binning, background parameterization for J/ψ …
Overall ~2x improvement

Impact on $H \to ZZ^* \to 4l$ Run 2 mass analysis

[Phys. Lett. B 843 (2023) 137880]

H→ZZ*→4l channel:

- Events containing at least four isolated leptons (l = e, μ) emerging from a common vertex, forming two pairs of oppositely charged same-flavour leptons
- 4 channels: $4\mu,\ 2e2\mu,\ 2\mu 2e,\ 4e$

- All the updates on the μ **systematic uncertainties** are propagated to the *4l* mass analysis
- For **e**, the analysis used previous calibration [arXiv:1812.03848]

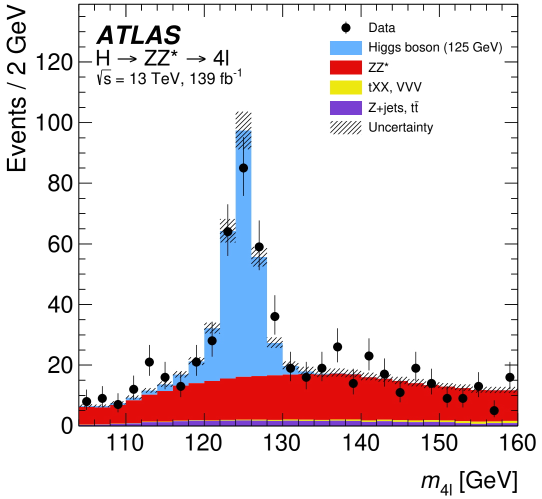

The analysis has always been stat. dominated

$$m_{H\to 4l,\mathrm{Run1}} = 124.51\pm0.52\ \mathrm{GeV} = 124.51\pm0.52\ \mathrm{(stat.)}\pm0.06\ \mathrm{(syst.)\ GeV}$$

$$m_{H\to 4l,\mathrm{Run2}} = 124.99\pm0.18\ \mathrm{GeV} = 124.99\pm0.18\ \mathrm{(stat.)}\pm0.04\ \mathrm{(syst.)\ GeV}$$

Systematic uncertainty on m_H $(H \to 4l)$	
Previous calibration	New calibration
60 MeV	**40 MeV**

~ 30% reduction!

Not negligible, becoming more and more important with the stat. increase